

Concise Synthesis and Biological Evaluation of 2-Aroyl-5-Amino Benzo[*b*]thiophene Derivatives As a Novel Class of Potent Antimitotic Agents

Romeo Romagnoli,^{*,†} Pier Giovanni Baraldi,^{*,†} Carlota Lopez-Cara,[†] Delia Preti,[†] Mojgan Aghazadeh Tabrizi,[†] Jan Balzarini,[‡] Marcella Bassetto,[§] Andrea Brancale,[§] Xian-Hua Fu,^{||} Yang Gao,^{||} Jun Li,^{||} Su-Zhan Zhang,^{||} Ernest Hamel,[⊥] Roberta Bortolozzi,[#] Giuseppe Basso,[#] and Giampietro Viola^{*,#}

[†]Dipartimento di Scienze Chimiche e Farmaceutiche, Università di Ferrara, 44121 Ferrara, Italy

[‡]Laboratory of Virology and Chemotherapy, Rega Institute for Medical Research, Minderbroedersstraat 10, B-3000 Leuven, Belgium

[§]School of Pharmacy and Pharmaceutical Sciences, Cardiff University, King Edward VII Avenue, Cardiff CF10 3NB, U.K.

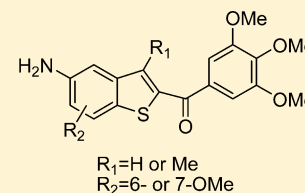
^{||}Cancer Institute, Key Laboratory of Cancer Prevention and Intervention, China National Ministry of Education, The Second Affiliated Hospital, School of Medicine, Zhejiang University, Hangzhou, Zhejiang Province 310009, People's Republic of China

[⊥]Screening Technologies Branch, Developmental Therapeutics Program, Division of Cancer Treatment and Diagnosis, Frederick National Laboratory for Cancer Research, National Cancer Institute, National Institutes of Health, Frederick, Maryland 21702, United States

[#]Dipartimento di Salute della Donna e del Bambino, Laboratorio di Oncoematologia, Università di Padova, 35131 Padova, Italy

S Supporting Information

ABSTRACT: The biological importance of microtubules make them an interesting target for the synthesis of antitumor agents. The 2-(3',4',5'-trimethoxybenzoyl)-5-aminobenzo[*b*]thiophene moiety was identified as a novel scaffold for the preparation of potent inhibitors of microtubule polymerization acting through the colchicine site of tubulin. The position of the methoxy group on the benzo[*b*]thiophene was important for maximal antiproliferative activity. Structure–activity relationship analysis established that the best activities were obtained with amino and methoxy groups placed at the C-5 and C-7 positions, respectively. Compounds **3c–e** showed more potent inhibition of tubulin polymerization than combretastatin A-4 and strong binding to the colchicine site. These compounds also demonstrated substantial antiproliferative activity, with IC₅₀ values ranging from 2.6 to 18 nM in a variety of cancer cell lines. Importantly, compound **3c** (50 mg/kg), significantly inhibited the growth of the human osteosarcoma MNNG/HOS xenograft in nude mice.



■ INTRODUCTION

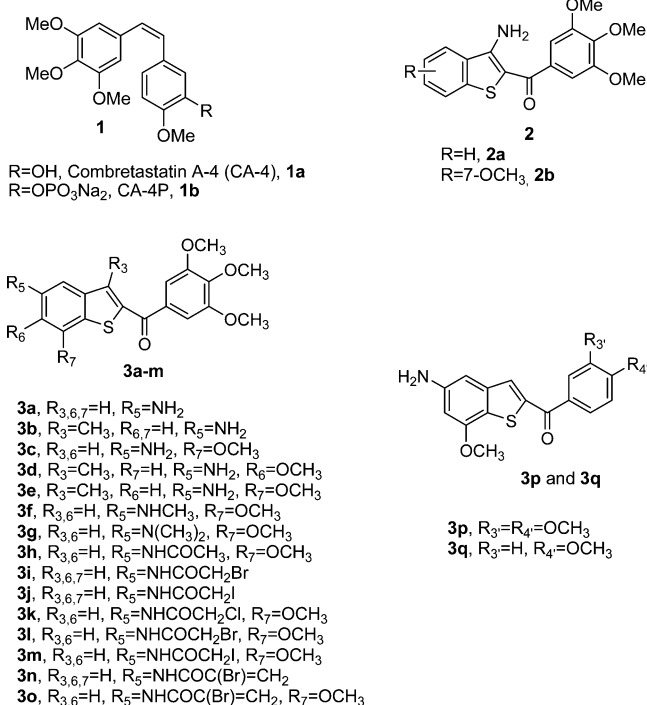
Microtubules are essential in a variety of cellular processes, including motility and signaling, separation of duplicated chromosomes during cell division, shape maintenance, and intracellular transport.^{1–3} The crucial involvement of microtubules in mitosis makes them an important target for anticancer drugs.^{4–6}

A large number of chemically diverse substances that interfere with the formation of the mitotic spindle have been identified.^{7,8} The natural stilbene derivative combretastatin A-4 (CA-4, **1a**, Chart 1), isolated by Pettit and co-workers from the bark of the South African tree *Combretum caffrum*,⁹ inhibits microtubule assembly by interacting with tubulin at the colchicine binding site.¹⁰ To improve the water solubility of CA-4, its disodium phosphate salt (CA-4P, **1b**) was synthesized¹¹ and CA-4P has yielded promising results in human clinical trials as a potent vascular disrupting agent (VDA).^{12–14}

Among the synthetic small molecules that inhibit tubulin assembly, we reported a class of 2-(3',4',5'-trimethoxybenzoyl)-3-aminobenzo[*b*]thiophene methoxy-substituted analogues with chemical formula **2**. The methoxy substitution and location on the benzene part of the benzo[*b*]thiophene moiety plays an important role in affecting tubulin polymerization and antiproliferative activity, with the most favorable position for the substituent being C-6 or C-7, while the C-4 and C-5 isomers were inactive.¹⁵ While the unsubstituted derivative **2a** was modestly active as an antiproliferative agent, with IC₅₀ values ranging from 0.29 to 1.8 μM against five cancer cell lines, compound **2b**, with a methoxy group at the 7-position, had potent activity (IC₅₀ = 9.5–33 nM). These compounds inhibited tubulin assembly and blocked the K562 cell cycle in the G2/M phase. These encouraging data led us to continue our research on this series of derivatives.

Received: September 10, 2013

Published: October 28, 2013

Chart 1. Chemical Structures of CA-4, CA-4P, and 2-Aroylbenzo[*b*]thiophene Derivatives 2a–b and 3a–q

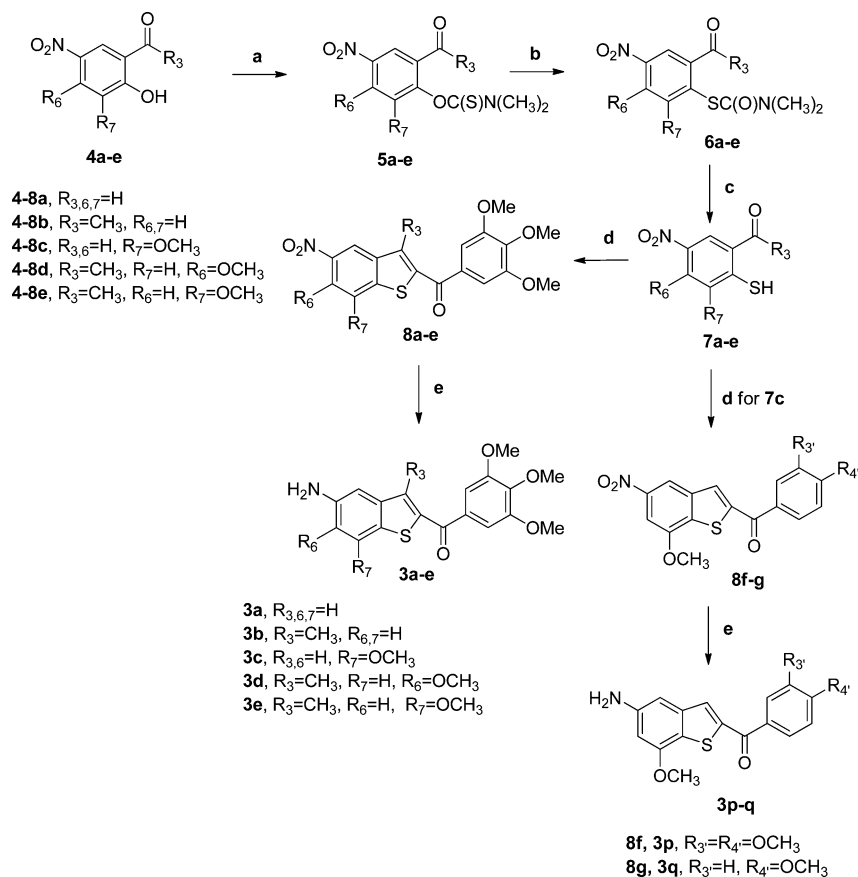
Our first goal in the studies presented here was to determine how important the amino substituent at the C-3 position was for activity. We found that simply shifting the amino group of derivative **2a** from the C-3 to the C-5 position of the benzo[*b*]thiophene nucleus to furnish derivative **3a** resulted in an 11–67-fold increase in potency (IC₅₀ = 0.78–18 nM, Table

1). This finding led us to undertake a more extensive structure–activity analysis of this scaffold in an effort to further increase antiproliferative activity, but no additional dramatic improvements were observed. We next prepared the 2-(3',4',5'-trimethoxybenzoyl)-5-aminobenzo[*b*]thiophene derivatives **3b–e** to explore the effects of the concomitant presence of a methyl group at the C-3 position or a methoxy moiety at the C-6 or C-7 positions. To understand the effect of alkyl substitution on the amino function of compound **3c**, *N*-methylamino and *N,N*-dimethylamino substituted analogues **3f** and **3g** were synthesized. The importance of the basicity of the amine function was evaluated by the synthesis of **3h**, the *N*-acetyl analogue of compound **3c**. Compounds **3i–o**, characterized by the presence of a haloacetyl amino or a α -bromoacryloylamino moiety at the 5-position of the benzo[*b*]thiophene ring, were synthesized because previous studies had shown that the electrophilic nature of the haloacetyl moiety sometimes improved compound activity.^{16,17} Moreover, the alkylation of sulfhydryl groups of tubulin by iodoacetamide¹⁸ and the disruption of microtubules by *p*-bromophenacyl bromide¹⁹ have been reported, with significant inhibitory effects on tubulin assembly. These derivatives were prepared by taking advantage of the low chemical reactivity as an alkylating moiety of the α -bromoacryloyl group. Regarding the chemical reactivity of the α -acrylic moiety, we speculated that an intracellular biological nucleophile could perform a first-step Michael attack on the double bond, possibly followed by a further reaction of the halogen α to the carbonyl, leading to a β elimination or a second nucleophilic substitution.²⁰ Finally, in an effort to further confirm whether the 3,4,5-trimethoxybenzoyl moiety at the 2-position of the benzo[*b*]thiophene nucleus of compound **3c** is important for antiproliferative activity, the 3',4'-dimethoxybenzoyl and 4'-methoxybenzoyl derivatives **3p** and **3q**, respectively, were prepared.

Table 1. In Vitro Growth Inhibitory Activity of Compounds 2a–b, 3a–o, and CA-4 (1a) against a Panel of Murine and Human Cancer Cells Lines

compd	IC ₅₀ (nM) ^a				
	L1210	FM3A/0	Molt4/C8	CEM/0	HeLa
2a	350 ± 32	1800 ± 300	290 ± 10	310 ± 20	nd
2b	33 ± 29	27 ± 13	8.5 ± 1.4	8.9 ± 2.0	nd
3a	0.78 ± 0.05	2.8 ± 0.2	18 ± 0.0	11 ± 0.7	13 ± 4
3b	8.0 ± 2.2	200 ± 12	100 ± 8	72 ± 1	100 ± 40
3c	5.0 ± 0.42	12 ± 5	2.6 ± 0.0	4.1 ± 1.6	8.0 ± 3.1
3d	19 ± 1	17 ± 1	16 ± 1	19 ± 2	16 ± 1
3e	12 ± 7	15 ± 0.0	14 ± 1	14 ± 2	13 ± 0.0
3f	67 ± 22	190 ± 10	74 ± 10	72 ± 14	66 ± 9
3g	1100 ± 60	1100 ± 70	980 ± 60	940 ± 63	360 ± 40
3h	340 ± 30	340 ± 10	98 ± 6	95 ± 8	69 ± 6
3i	1400 ± 300	1700 ± 100	960 ± 82	260 ± 40	1600 ± 200
3j	1400 ± 200	2100 ± 200	330 ± 40	330 ± 30	1500 ± 100
3k	80 ± 22	200 ± 12	78 ± 4	72 ± 1	100 ± 40
3l	420 ± 10	250 ± 21	360 ± 20	340 ± 30	220 ± 20
3m	410 ± 50	370 ± 10	330 ± 10	310 ± 10	200 ± 19
3n	75 ± 4	170 ± 0.0	270 ± 10	140 ± 70	700 ± 21
3o	96 ± 9	200 ± 30	280 ± 12	260 ± 90	760 ± 71
3p	1900 ± 500	2200 ± 400	1700 ± 300	1400 ± 300	1600 ± 600
3q	>10000	>10000	6500 ± 600	6100 ± 200	6300 ± 800
CA-4 (1a)	2.8 ± 1.1	42 ± 6.0	16 ± 1.4	1.9 ± 1.6	1.9 ± 1.6

^aIC₅₀ = compound concentration required to inhibit tumor cell proliferation by 50%. Data are expressed as the mean ± SE from the dose–response curves of at least three independent experiments. nd = not determined.

Scheme 1^a

^aReagents and conditions: (a) ClC(S)N(CH₃)₂, DABCO, DMF, 50 °C, 5 h; (b) toluene, reflux; (c) NaOH, EtOH/H₂O, 65 °C; (d) 3,4,5-trimethoxyphenyl-2-bromoethanone for **7a–e**, 3,4-dimethoxyphenyl-2-bromoethanone and 4-methoxyphenyl-2-bromoethanone for **7e**, K₂CO₃, (CH₃)₂CO, reflux; (e) SnCl₂·2H₂O, EtOH, reflux.

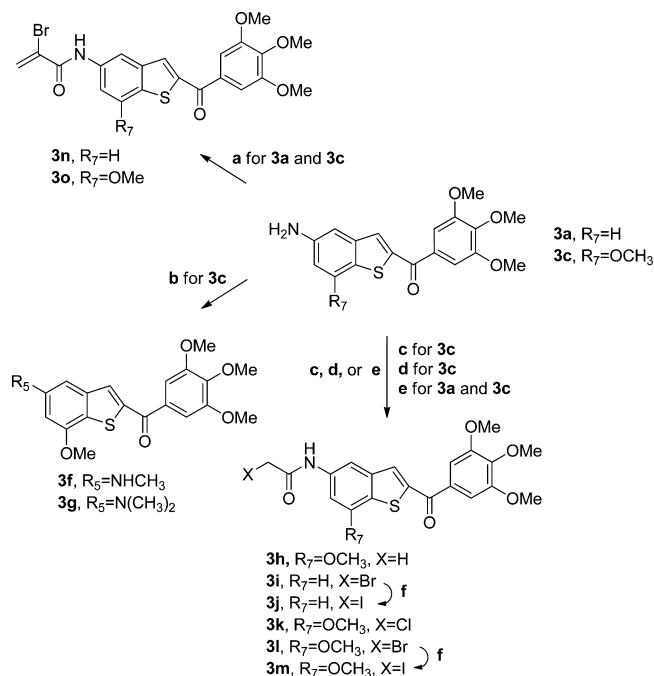
CHEMISTRY

The 2-(3',4',5'-trimethoxybenzoyl)-5-aminobenzo[*b*]thiophene derivatives **3a–e** were synthesized by the five-step synthesis shown in Scheme 1. Starting from the variously substituted 5-nitro salicylaldehydes **4a** and **4c** or 5-nitro-2-hydroxyacetophenones **4b** and **4d–e**,²¹ the reaction with *N,N*-dimethylthiocarbonyl chloride in *N,N*-dimethylformamide in the presence of DABCO yielded the *O*-arylthiocarbamates **5a–e** in good yields. These latter were submitted to Newman–Kwart rearrangement²² in a refluxing toluene solution to furnish the corresponding *S*-arylthiocarbamates **6a–e**. The subsequent hydrolysis using a 3 M aqueous NaOH solution furnished the desired 2-thiophenols **7a–e**, which were used without further purification for the next reaction. The 5-nitrobenzo[*b*]thiophene derivatives **8a–e** were synthesized by a “one-pot” cyclization reaction of the thiophenols **7a–e** with 2-bromo-1-(3',4',5'-trimethoxyphenyl)ethanone and K₂CO₃ in refluxing acetone. The reduction of the nitro group with SnCl₂ in refluxing ethanol furnished the corresponding amino derivatives **3a–e**. Compounds **8f** and **8g** were prepared by the “one-pot” condensation from **7c** and the corresponding α -bromoacetophenone, followed by reduction of the 5-nitro group, to yield the 5-amino derivatives **3p** and **3q**, respectively. The C-5 amino derivative **3c** was converted into the *N*-methylamino and *N,N*-dimethylamino derivatives **3f** and **3g**, respectively, by reaction with CH₃I in the presence of K₂CO₃ and DMF.

Acetylating or haloacetylating the 5-amino group of **3a** and **3c** with acetyl chloride, chloroacetyl chloride, and bromoacetyl chloride in the presence of pyridine provided the acetamide (**3h**), chloroacetamide (**3k**), and bromoacetamide (**3i** and **3l**) derivatives, respectively. The iodoacetyl derivatives **3j** and **3m** were prepared from the bromoacetyl derivatives **3i** and **3l** by an exchange reaction using NaI in DMA. Finally, the α -bromoacryloylamido derivatives **3n** and **3o** were obtained by the coupling of α -bromoacrylic acid with the corresponding 5-aminobenzo[*b*]thiophene derivatives **3a** and **3c** in dry DMF, using EDCI as the condensing agent (Scheme 2).

BIOLOGICAL RESULTS AND DISCUSSION

In Vitro Antiproliferative Activities. Table 1 summarizes the growth inhibitory effects of the new 5-substituted benzo[*b*]thiophene derivatives **3a–q** against two types of murine cancer cell lines, leukemia L1210 and mammary carcinoma FM3A cells, as well as three types of human cancer cell lines, T-lymphoblastoid leukemia (Molt/4 and CEM) and cervix carcinoma HeLa cells, in comparison with the 3-aminobenzo[*b*]thiophenes **2a–b** and CA-4 (**1a**) as reference compounds. Among the evaluated compounds, derivatives **3a**, **3c**, **3d**, and **3e** showed the most potent antiproliferative activity, with IC₅₀ values of 0.78–18, 2.6–12, 16–19, and 12–15 nM, respectively. The four compounds were thus more potent than CA-4 against the FM3A cells, while **3c** was also more active than CA-4 against the Molt/4 cells. Compounds **3a**, **3c**, **3d**, and

Scheme 2^a

^aReagents and conditions: (a) α -bromoacrylic acid, EDCl, DMF, rt; (b) MeI, K₂CO₃, DMF; (c) CH₃COCl, Py, CH₂Cl₂, rt; (d) ClCH₂COCl, Py, CH₂Cl₂, rt; (e) BrCH₂COBr, Py, CH₂Cl₂, rt; (f) NaI, CH₃CON(CH₃)₂, rt.

3e were less active than CA-4 against CEM and HeLa cells. Only **3a** was more potent than CA-4 against the L1210 cells.

Moving the amino group from the C-3 to the C-5 position of the benzo[*b*]thiophene ring (**3a** vs **2a**, **3c** vs **2b**) significantly increased antiproliferative activity, as noted in the Introduction for **3a** vs **2a**. Thus, in these two examples, the amino group located on the benzene portion of the benzo[*b*]thiophene nucleus is preferable to its location on the thiophene part of the molecule. Compound **3a** was more active against the two murine cell lines as compared with the three human cancer cell lines. In contrast, the activity of **3c** was more uniform across the five cell lines, and, perhaps more importantly, **3c** was more active than **3a** in the three human cell lines. This perhaps resulted from the introduction of a methoxy group at the C-7 position of the benzo[*b*]thiophene nucleus in **3c** as compared with **3a**.

Compound **3b**, with a methyl group at the C-3 position of derivative **3a**, showed a reduction in antiproliferative activity by 6–71-fold as compared with **3a**, with the greatest difference being with the FM3A cells. Comparing **3b** with **2a**, except for the concomitant introduction of the NH₂ moiety at C-5 in the former compound, it may be that a methyl group at C-3 is superior to the amino group at this position. Comparing the 3-methyl-7-methoxy derivative **3e** with the 3-unsubstituted analogue **3c**, there was a 1.3–5-fold decrease in antiproliferative activity in the five cell lines studied. Finally, the cell growth inhibitory activities of compounds **3d** and **3e** were very similar, indicating that placing a methoxy group at the C-6 (**3d**) or C-7 (**3e**) position of the 3-methyl benzo[*b*]thiophene nucleus had similar effects, while comparing **3d** with **3c** reinforces the **3b/3a** finding that the C-3 methyl group was deleterious for antiproliferative activity.

Compounds **3f–h** and **3i–o** were designed to test the effects of alkylation and haloalkylation, respectively, of the C-5 amino group, with and without the C-7 methoxy group. These compounds all had significantly reduced antiproliferative activity as compared with **3a** and **3c–e**, although several had activity comparable with or greater than that of compound **2a**. This group included the more active **3f**, **3h**, and **3k** and the less active **3l–o**. Of these compounds, all except **3n** possessed the C-7 methoxy moiety. Overall, these data support the idea that the C-5 amino group acts as a hydrogen bond donor rather than an acceptor.

Finally, we wished to confirm what we had previously observed with related compounds, that the trimethoxyphenyl ring is required for activity.¹⁵ We therefore took the **3c** scaffold, with both the C-5 NH₂ and C-7 methoxy moieties, and eliminated either one (**3p**) or two (**3q**) methoxy groups on the trimethoxyphenyl ring. Both compounds had much reduced antiproliferative activity, as we had observed before.¹⁵

Evaluation of Cytotoxicity in Noncancer Cells. To investigate the antiproliferative activities of these new derivatives in normal human cells, compound **3c** was tested in vitro against peripheral blood lymphocytes (PBL) isolated from healthy donors (Table 2) and human umbilical vein

Table 2. Cytotoxicity of **3c** in Human Peripheral Blood Lymphocytes (PBL) and in HUVEC

	IC ₅₀ (μM) ^a
	3c
PBL _{resting} ^b	24.7 ± 4.6
PBL _{PHA} ^c	20.6 ± 4.8
HUVEC	5.5 ± 1.1

^aCompound concentration required to reduce cell growth by 50%. Values are the mean ± SEM for three independent experiments. ^bPBL not stimulated with PHA. ^cPBL stimulated with PHA.

endothelial cells (HUVECs). After treatment of both resting and PHA-stimulated lymphocytes for 72 h, the IC₅₀ values were over 20 μM, indicating that **3c** did not substantially affect the viability of these cells. Relatively low toxicity (IC₅₀, 5.5 μM) was observed for **3c** with HUVECs, which were 460–2100-fold less sensitive than the cancer cell lines. Altogether, these data suggest that **3c** has cancer cell selective killing properties.

Inhibition of Tubulin Polymerization and Colchicine Binding. To investigate whether these 5-aminobenzo[*b*]thiophene derivatives interacted with tubulin, compounds **3a–e** were selected to evaluate inhibitory effects on tubulin polymerization and measure their ability to compete for the colchicine binding site (Table 3).²³ CA-4 and 3-aminobenzo[*b*]thiophene derivatives **2a–b** were evaluated as reference compounds. 5-Aminobenzo[*b*]thiophenes **3a–e** strongly inhibited tubulin assembly, and derivatives **3c**, **3d**, and **3e**, with IC₅₀ values of 0.58, 0.68, and 0.48 μM, respectively, were about as effective as CA-4 (IC₅₀, 1.2 μM), while **3b** had an IC₅₀ value of 1.3 μM, comparable to that of CA-4. Compounds **2b**, **3a**, and **2a** were progressively less active than CA-4. Thus, the order of inhibitory effects on tubulin polymerization was **3e** = **3c** > **3d** > **3b** = CA-4 > **2b** > **3a** > **2a**.

The results suggest that antiproliferative activity was correlated with tubulin polymerization inhibition. We observed a good correlation for compounds **3c**, **3d**, and **3e**, but not for **3a** and **3b**. Thus, while compounds **3c**, **3d**, and **3e** were the best inhibitors of tubulin assembly, their inhibitory effects on cancer

Table 3. Inhibition of Tubulin Polymerization and Colchicine Binding by Compounds 2a–b, 3a–e, and CA-4

compd	tubulin assembly ^a IC ₅₀ ± SD (μM)	colchicine binding ^b % ± SD	
		5 μM drug	1 μM drug
2a	4.2 ± 0.7	39 ± 9	nd ^c
2b	2.1 ± 0.09	39 ± 1	nd
3a	3.2 ± 0.1	65 ± 0.2	nd
3b	1.3 ± 0.07	78 ± 2	nd
3c	0.52 ± 0.04	97 ± 1	89 ± 3
3d	0.68 ± 0.06	95 ± 1	83 ± 4
3e	0.48 ± 0.01	95 ± 2	90 ± 4
CA-4 (1a)	1.2 ± 0.2	99 ± 0.5	88 ± 1

^aInhibition of tubulin polymerization. Tubulin was at 10 μM.

^bInhibition of [³H]colchicine binding. Tubulin and colchicine were at 1 and 5 μM, respectively. ^cnd: not determined

cell growth were matched by those of derivative 3a, which was 6-fold less active as an assembly inhibitor. However, this discrepancy in antitubulin versus antiproliferative activity is not infrequently observed for antimetabolic agents. The most reasonable explanation is that, in the tubulin polymerization assay, the composition of bovine brain tubulin, in terms of tubulin isotypes, differs significantly from that of different human cancer cell lines.²⁴

In the colchicine competition assay, compounds 3a–e strongly bound to the [³H]colchicine binding domain of tubulin because 65–98% inhibition occurred with these agents and colchicine both at 5 μM.²⁵ Compounds 3c–e were the most active inhibitors of the binding reaction because 83–90% and 95–97% inhibition occurred with these agent at 1 and 5 μM, respectively. At these concentrations, derivatives 3c–e were as active as CA-4, which in these experiments inhibited colchicine binding by 99% and 88% at 5 and 1 μM, respectively. Inhibition of colchicine binding by compounds 3a and 3b was lower at 5 μM, with 65% and 78% inhibition occurring with these agents. These results suggest that the antiproliferative activity of these compounds resulted from inhibition of tubulin polymerization by binding at the colchicine site. In general, in these experiments, inhibition of tubulin assembly correlated more closely with inhibition of [³H]colchicine binding to tubulin than did antiproliferative activity.

Molecular Modeling. We performed a series of molecular docking simulations to investigate the possible binding mode of this new series of molecules in the colchicine site of β-tubulin.²⁶ The results for the compounds studied (3a–e) show that all the structures docked with the trimethoxyphenyl ring in proximity to Cys241 and with the amino group establishing a hydrogen bond with Thr179 (Figure 1A). Interestingly, the methoxy group, either in position 6 or 7 of the benzo[*b*]-thiophene ring, allows a better occupancy of the binding pocket for compounds 3c–e by interacting closely with Met259, stabilizing the overall binding pose for these compounds. Furthermore, the methyl group present in 3b, 3d, and 3e establishes a hydrophobic interaction with Leu248 (Figure 1B). It should also be noted that the described binding mode for this series of compounds is very similar to the one observed for colchicine (see Supporting Information). Overall, the *in silico* results correlate well with the tubulin polymerization inhibition and colchicine binding experimental data.

Analysis of Cell Cycle Effects. The effects of a 24 h treatment with different concentrations of 3c on cell cycle

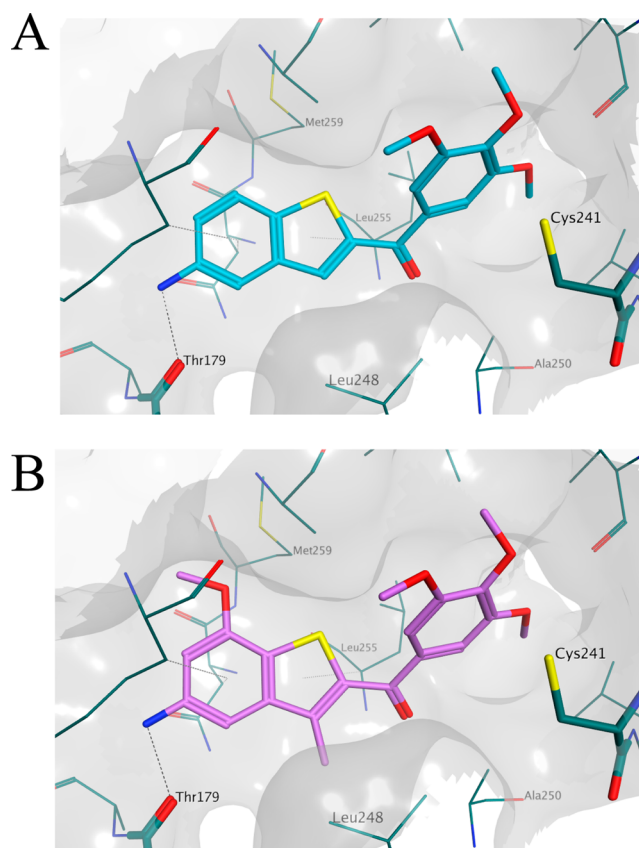


Figure 1. Proposed binding mode for compounds 3a (A) and 3e B), obtained by molecular docking simulation into the colchicine binding pocket of β-tubulin.

progression in HeLa and Jurkat cells were determined by flow cytometry (Figure 2A,B). The compound induced a remarkable G2/M arrest in a concentration-dependent manner in the cell lines tested, with an increase in G2/M cells occurring at a concentration as low as 10 nM, while at higher concentrations (15–30 nM), more than 80% of the HeLa and 40% of the Jurkat cells were blocked in G2/M. The increase in G2/M phase cells was accompanied by a dramatic reduction in S phase cells in both lines. There was excellent agreement between the potency in the inhibitory effects on tubulin polymerization by compound 3c and its remarkable ability to induce a G2/M arrest.

We further studied the correlation between 3c-induced G2/M arrest and alterations in expression of proteins that regulate cell division. The cdc2/cyclin B complex controls both entry into and exit from mitosis. Phosphorylation of cdc2 on Tyr15 and phosphorylation of cdc25c phosphatase on Ser216 negatively regulate the activation of the cdc2/cyclin B complex. Thus, dephosphorylation of these proteins is necessary to activate the cdc2/cyclin B complex and is mediated by the phosphatase cdc25c, which dephosphorylates cdc2 and autodephosphorylates itself. Phosphorylation of cdc25c directly stimulates both its phosphatase and autophosphatase activities, a condition required to trigger cdc2/cyclin B induction of entry of cells into mitosis.^{27–29} Thus, the protein level of cyclin B and the phosphorylation status of both cdc2 and cdc25c were examined by Western blot analysis. As shown in Figure 3, treatment with 3c in HeLa cells at either 10 or 100 nM caused no significant variations in cyclin B expression after either a 24 or 48 h treatment. In contrast, changes in the phosphorylation

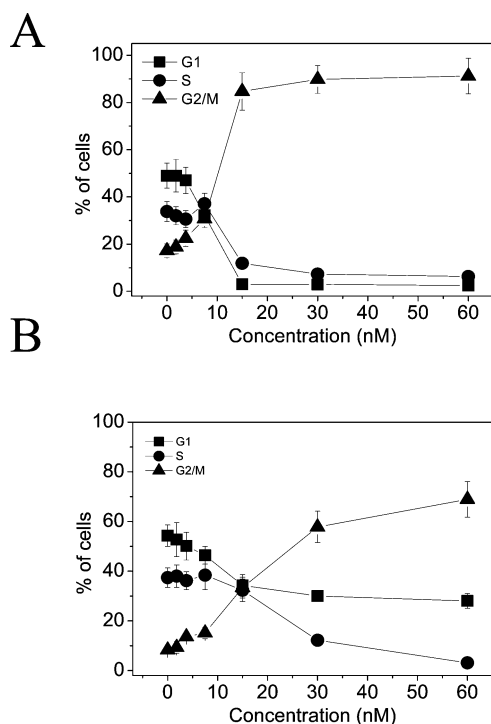


Figure 2. Percentage of cells in each phase of the cell cycle in HeLa (A) and Jurkat (B) cells, treated with 3c at the indicated concentrations for 24 h. Cells were fixed and labeled with PI and analyzed by flow cytometry as described in the Experimental Section. Data are presented as mean \pm SEM of three independent experiments.

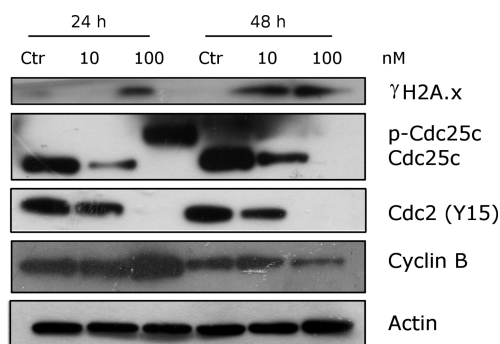


Figure 3. Effects of 3c on G2/M regulatory proteins and phosphohistone γ H2A.X. HeLa cells were treated for 24 or 48 h with 3c at the indicated concentrations. The cells were harvested and lysed for the detection of cyclin B, p-cdc2^{Y15}, cdc25C, and γ H2A.X expression by Western blot analysis. To confirm equal protein loading, each membrane was stripped and reprobed with an anti- β -actin antibody.

status of cdc25c were observed after 24 h of treatment along with a strong reduction in the expression of this protein. At 48 h, disappearance of the cdc25c persisted and the p-cdc25c formed at 24 h disappeared as well. We also observed a dramatic decrease in the expression of the phosphorylated form of cdc2 (Tyr15). These data, along with the fact that over 80% of the cells accumulated in the G2/M phase, suggest that 3c-induced G2/M arrest was not due to defects in G2/M regulatory proteins but, rather, is closely linked with acceleration of entry into mitosis.

Prolonged mitotic arrest can lead to DNA damage.³⁰ To identify DNA damage, we examined treated cells for the

appearance of the phosphorylated histone variant H2A.x (γ -H2A.X). Compound 3c at 100 nM induced a striking increase in the expression of γ -H2A.X after a 24 h treatment, while after 48 h γ -H2A.X became apparent also at 10 nM. This result confirms that 3c induced strong DNA damage during mitotic arrest and that this effect could contribute to its antiproliferative activity.

Compound 3c Induced Apoptosis. To evaluate the mode of cell death induced by 3c, a flow cytometric analysis was performed using propidium iodide (PI), which stains DNA and enters only dead cells, and the protein annexin-V, which selectively binds to apoptotic cells that expose on their surface the phospholipid phosphatidylserine.³¹ Thus, this analysis is able to distinguish between live cells (annexin-V⁻/PI⁻), early apoptotic cells (annexin-V⁺/PI⁻), late apoptotic cells (annexin-V⁺/PI⁺), and necrotic cells (annexin-V⁻/PI⁺). As shown in Figure 4A,B, HeLa cells treated with 3c for 24 h

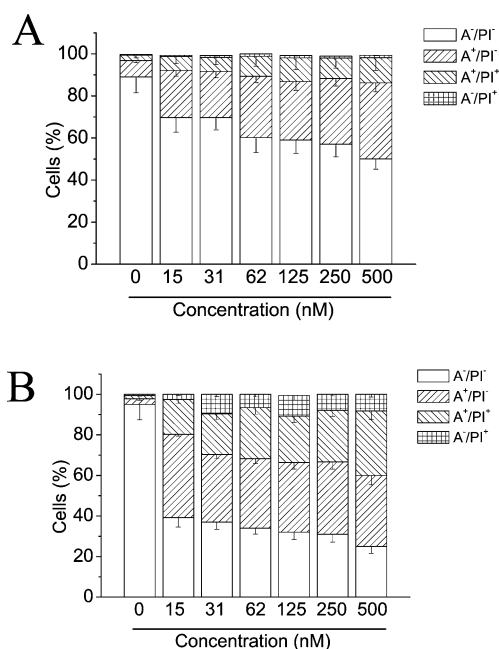


Figure 4. Flow cytometric analysis of apoptotic cells after treatment of HeLa cells with 3c at the indicated concentrations after incubation for 24 h (A) or 48 h (B). The cells were harvested and labeled with annexin-V-FITC and PI and analyzed by flow cytometry. Data are presented as mean \pm SEM of three independent experiments.

showed an accumulation of annexin-V positive cells in comparison with the control cells and the annexin-V positive cells further increased after 48 h. Apoptotic cells also increased in a concentration dependent manner, with an increase in the percentage of apoptotic cells observed at the lowest 3c concentration examined (15 nM).

Compound 3c Induced Mitochondrial Dysfunction. It is well-known that, as a result of apoptotic stimuli, alterations of the mitochondrial transmembrane potential ($\Delta\psi_{mt}$) are often observed³² and that the mitochondrial apoptotic pathway is induced following cell treatment with many antimetabolic agents.³³ Thus, to analyze the involvement of the mitochondria-initiated intrinsic pathway, we examined the mitochondrial membrane permeability of HeLa cells treated with 3c. $\Delta\psi_{mt}$ was monitored staining the cells with the fluorescent probe 5,5',6,6'-tetrachloro-1,1',3,3'-tetraethylbenzimidazol-carbocyanine (JC-1). As shown in Figure 5A, 3c induced a time and

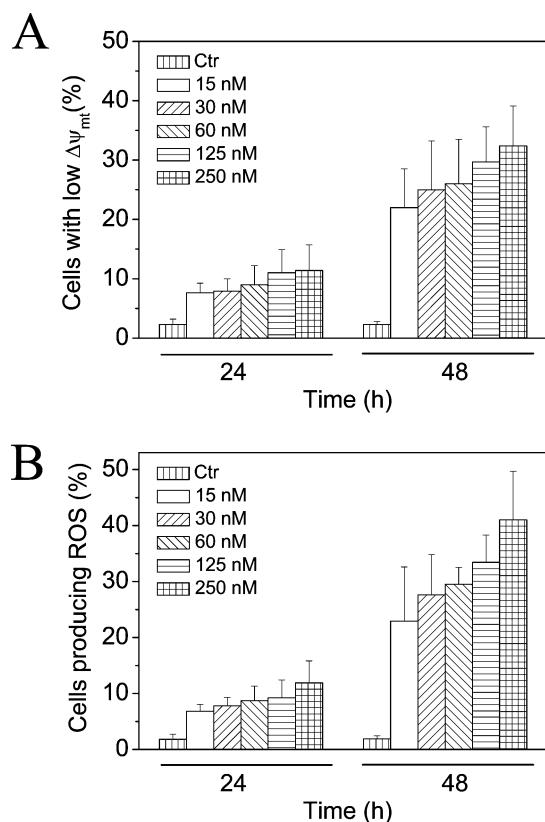


Figure 5. (A) Assessment of mitochondrial membrane potential ($\Delta\psi_{mt}$) after treatment of HeLa cells with 3c. Cells were treated with the indicated concentrations of 3c for 24 or 48 h and then stained with the fluorescent probe JC-1. Data are expressed as mean \pm SEM for three independent experiments. (B) Mitochondrial production of ROS in HeLa cells following treatment with compound 3c. After 24 or 48 h incubations with the indicated concentration of 3c, cells were stained with H_2 -DCFDA and analyzed by flow cytometry. Data are expressed as mean \pm SEM of three independent experiments.

concentration-dependent increase in the percentage of cells with depolarized mitochondria, and this effect correlated well with the induction of apoptosis described above.

It is also well-known that reduction of mitochondrial membrane potential is associated with mitochondrial production of reactive oxygen species (ROS).³⁴ In particular, with cytochrome *c* release from mitochondria, a shift from the normal four-electron reduction of O_2 to a one-electron reduction produces superoxide anion.^{34a} For that reason, we evaluated the intracellular level of ROS after treatment with 3c by flow cytometry utilizing the fluorescence indicator 2',7'-dichlorodihydrofluorescein diacetate (H_2 -DCFDA).³⁵ The results shown in Figure 5B indicated that 3c induced, in a time and concentration dependent manner, an increase of the intracellular level of ROS in comparison with untreated cells, which is in good agreement with the mitochondrial depolarization described above. Overall, these results suggest that 3c induced apoptosis follows the mitochondrial pathway.

Compound 3c Induced Caspase Activation. Caspase activation plays an essential role in the propagation of apoptosis.³⁶ Caspases are constitutively expressed as pro-enzymes that can be activated by a proteolytic cleavage at specific sites. Caspases-2, -8, -9, and -10 are called activator caspases and usually are the initiators of the apoptotic process. Furthermore, mitochondrial depolarization results in the efflux

of certain proteins and small molecules, such as cytochrome *c*. Once cytochrome *c* is released in the cytoplasm, it binds to procaspase-9, forming the so-called apoptosome, which subsequently stimulates proteolytic activation of caspase-3.³⁷ As shown in Figure 6, compound 3c induced proteolytic

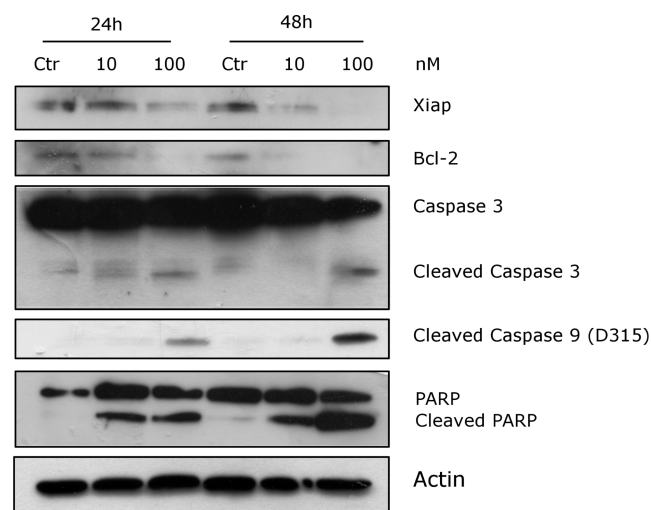


Figure 6. Effect of 3c on caspase activation and on Bcl-2 and Xiap expression in HeLa cells. Cells were treated for 24 or 48 h with 3c at the indicated concentrations. The cells were harvested and lysed for the detection of cleaved caspase-9, pro-caspase-3, PARP, Bcl-2, and Xiap expression by Western blot analysis. To confirm equal protein loading, each membrane was stripped and reprobed with an anti- β -actin antibody.

cleavage of caspase-9 and caspase-3, in good agreement with the mitochondrial depolarization described above. The DNA repair enzyme poly(ADP-ribose) polymerase (PARP) is cleaved by caspase-3 from its full length 116 kDa form to an inactive 85 kDa form, and, accordingly, we also observed that PARP cleavage was detectable at 24 h and at a low concentration (10 nM) of 3c. Altogether, these results showed that 3c-induced apoptosis is caspase-dependent.

Effect of 3c on Bcl-2 and XIAP Expression. It is well-known that antimicrotubule compounds affect signaling pathways that involve the regulation of the Bcl-2 family of proteins.^{33a} Bcl-2 is an antiapoptotic member of the Bcl-2 protein family and is one of the main regulators of the mitochondrial apoptotic pathway. Moreover, it is located in the outer mitochondrial membrane and protects cells from apoptosis through the control of mitochondrial permeability and release of cytochrome *c*.³⁸ Many microtubule inhibitors, such as vincristine, colchicine, and paclitaxel, induce the Bcl-2 downregulation that ultimately leads to apoptotic cell death.³⁹ As shown in Figure 6, the expression of Bcl-2 was strongly reduced in HeLa cells following treatment with 3c at both concentrations examined (10 and 100 nM).

Xiap is a member of the IAP family (inhibitors of apoptosis protein). In general, the IAPs suppress cell death response through a direct interaction with caspases, including caspase-3, caspase-7, and caspase-9, inhibiting their processing and activation.⁴⁰ We found (Figure 6) that expression of Xiap was strongly downregulated after both 24 and 48 h treatments with 3c, even with only 10 nM 3c. Moreover, this effect was concurrent with activation of the caspases.

In Vivo Antitumor Activity of Compound 3c. The antitumor activity of 3c was evaluated in vivo using a human

osteosarcoma xenograft model in Balb/C-nu nude mice. In preliminary experiments *in vitro*, we determined that compound **3c** showed potent cytotoxic activity ($IC_{50} = 1.0 \pm 0.1$ nM) against the human osteosarcoma cell line MNNG/HOS. Once the MNNG/HOS xenografts reached a size of ~ 100 mm³, 12 mice were randomly assigned to one of three groups. In two of the groups, compound **3c**, dissolved in 5% (v/v) DMSO/olive oil, or reference compound CA-4P (**1b**), dissolved in isotonic saline, were injected intraperitoneally at a dose of 50 mg/kg. Both drugs, as well as the vehicle control, were administered four times, once every three days. As shown in Figure 7A, even the first dose of compound **3c** induced a

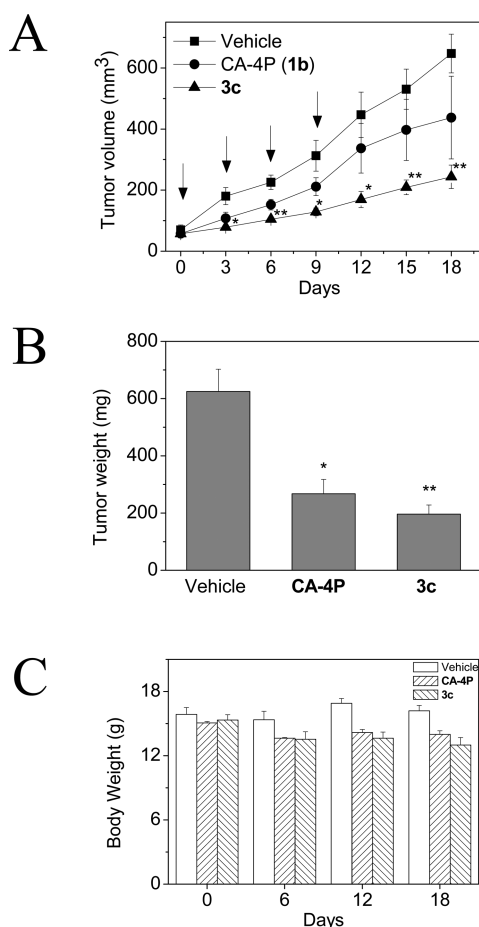


Figure 7. Inhibition of human xenograft growth *in vivo* by compound **3c**. (A) MNNG/HOS human osteosarcoma tumor-bearing nude mice were administered the vehicle, as controls, or 50 mg/kg of **3c** or CA-4P (**1b**). Injections were given intraperitoneally on days 0, 3, 6, and 9 (indicated by arrows). The figure shows the average measured tumor volumes (A), the weight of the excised tumor at the end of the observation period (B), and the body weights of the mice recorded on the indicated days after treatments (C). Data are expressed as mean \pm SEM of tumor volume, tumor weight, and body weight at each time point for three animals per group. * $p < 0.05$ and ** $p < 0.01$ vs. control.

significant reduction in tumor growth, reaching a 62% reduction by the end of the observation period (18th day), as compared with administration of vehicle only. As early as the day after the second dose of **3c**, the reduction in tumor growth was statistically significant, indicating a fast and efficient delivery of compound to the tumor mass. The effect of **3c** on the reduction in tumor volume was greater than that of **1b**,

which caused a 32% reduction at day 18. When the observation time ended, the animals were sacrificed and the tumors excised and weighed. The results (Figure 7B again showed a statistically significant reduction in tumor weight in the **3c** treated animals. Although not as great as the tumor weight reduction with **3c**, a statistically significant weight reduction was also observed for the animals treated with **1b**.

No significant weight changes were observed in the treated animals during the entire treatment period (Figure 7C), suggesting that **3c** induced minimal toxicity.

CONCLUSIONS

Wanting to verify that the *ortho*-relationship between the 3',4',5'-trimethoxybenzoyl and amino moieties in derivatives with general structure **2** was essential for their activity, we found instead that moving the amino group from the C-3 to the C-5 position of the benzo[*b*]thiophene nucleus led to a consistent increase in antiproliferative activity. Thus, compound **3a**, with the amino group at the C-5 position of the benzo[*b*]thiophene ring, showed a 16–640-fold increased improvement in IC_{50} values over its C-3 amino analogue **2a** in four cancer cell lines. SAR studies with the available analogues demonstrated, particularly in the three human cancer cell lines, that antiproliferative activity was enhanced with the electron-donating methoxy substituent at the C-7 and possibly at the C-6 position on the benzo[*b*]thiophene nucleus and was reduced by the presence of a methyl group at the C-3 position. The C-3 methyl derivatives **3b** and **3e** showed reduced antiproliferative activity compared with their corresponding C-3 unsubstituted counterparts **3a** and **3c**. However, the available analogues also suggest that a C-3 methyl group is more favorable to activity than the original C-3 amino moiety. Four compounds (**3a**, **3c**, **3d**, and **3e**) displayed strong antiproliferative activity with IC_{50} values lower than 100 nM against the panel of cancer cell lines. By alkylation of the C-5 amino group, we confirmed that this moiety is essential for activity and molecular modeling indicated formation of a stabilizing hydrogen bond with Thr179 of β -tubulin. We also found that the 3,4,5-trimethoxybenzoyl substitution at the C-2 position was essential for potent antiproliferative activity. The molecular models indicated that this moiety, like the analogous moiety of CA-4 and colchicine, interacted with Cys241 of β -tubulin. Compounds **3c–e** had activities higher than that of CA-4 as inhibitors of tubulin polymerization and also potently inhibited the binding of [³H]colchicine to tubulin, in agreement with the molecular models. Considering that toxicity is a major factor that limits the effectiveness of antimitotic agents, the results obtained with compound **3c** on noncancer cells (PBL and HUVEC) suggest that **3c** may not interfere greatly with microtubule dynamics in normal cells. These cellular studies seemed to be corroborated by the limited toxicity (minimal weight loss) we observed in tumor-bearing mice treated with **3c**, even as the cancers shrank dramatically. Further cellular studies showed that the induction of apoptosis by **3c** was associated with dissipation of the mitochondrial transmembrane potential, activation of caspase-9 and caspase-3, and other terminal events of apoptosis such as PARP cleavage. In conclusion, our results demonstrated that **3c** is a very promising new tubulin binding agent, and its initial strong *in vivo* antitumor activity demonstrates that it warrants further preclinical evaluation.

EXPERIMENTAL SECTION

Chemistry. Materials and Methods. All commercially available solvents and reagents were used without further purification. Melting points were recorded on a Buchi-Tottoli apparatus and are uncorrected. All reactions were monitored using TLC on silica gel F₂₅₄ plates, and compounds were visualized with aqueous KMnO₄. Flash chromatography was performed using commercial silica gel (230–400 mesh). ¹H NMR data were obtained in CDCl₃ or as specified with a Varian VXR 200 spectrometer or a Varian Mercury Plus 400 spectrometer. Peak positions are given in ppm (δ) downfield, and *J* values are given in hertz. Electron spray ionization (ESI) mass spectra were obtained on a double-focusing Finnigan MAT 95 spectrometer. The purity of tested compounds was determined by combustion elemental analyses conducted by the Microanalytical Laboratory of the Chemistry Department of the University of Ferrara with a Yanagimoto MT-5 CHN recorder elemental analyzer. All tested compounds yielded data consistent with a purity of at least 95% as compared with the theoretical values.

General Procedure A for the Synthesis of Compounds 5a–e.

To a solution of 5-nitrosalicylaldehydes **4a** and **4c** or 5-nitro-2-hydroxyacetophenones **4b** and **4d–e** (5 mmol) in DMF (30 mL) containing DABCO (1.14 g, 10 mmol) was added *N,N*-dimethylthiocarbamoyl chloride (0.94 g, 7.6 mmol) in one portion. The temperature rose rapidly to 50 °C, and the mixture was stirred at this temperature for 5 h. After this time, water was added (30 mL) and the mixture was extracted with CH₂Cl₂ (3 × 30 mL). The organic phase was washed with 5% HCl (20 mL), 1 M NaOH (20 mL), and brine (20 mL), dried over Na₂SO₄, and evaporated in vacuo. The crude product was purified by column chromatography on silica gel or recrystallized from petroleum ether.

O-2-Formyl-4-nitrophenyl-*N,N*-dimethylcarbamothioate (5a). Using general procedure A, the crude product purified by crystallization from petroleum ether yielded **5a** as a yellow solid; yield 91%; mp 81–83 °C. ¹H NMR (CDCl₃) δ: 3.03 (s, 3H), 3.19 (s, 3H), 7.78 (d, *J* = 8.4 Hz, 1H), 8.36 (dd, *J* = 8.4 and 2.6 Hz, 1H), 8.76 (d; *J* = 2.8 Hz, 1H), 10.3 (s, 1H). MS (ESI): [M + 1]⁺ = 255.1.

O-2-Acetyl-4-nitrophenyl-*N,N*-dimethylcarbamothioate (5b). Using procedure A, the crude product was purified by column chromatography with EtOAc–petroleum ether 3:7 as eluent to give **5b** as a yellow oil; yield 95%. ¹H NMR (CDCl₃) δ: 2.61 (s, 3H), 2.87 (s, 3H), 2.95 (s, 3H), 7.26 (d, *J* = 8.8 Hz, 1H), 8.36 (dd, *J* = 8.8 and 2.4 Hz, 1H), 8.62 (d; *J* = 2.4 Hz, 1H). MS (ESI): [M + 1]⁺ = 269.2.

O-2-Formyl-4-nitro-6-methoxyphenyl-*N,N*-dimethylcarbamothioate (5c). Using procedure A, the crude product was purified by crystallization from petroleum ether to give the product **5c** as a yellow solid; yield 91%; mp 129–131 °C. ¹H NMR (CDCl₃) δ: 3.45 (s, 3H), 3.48 (s, 3H), 3.97 (s, 3H), 8.00 (d, *J* = 2.4 Hz, 1H), 8.39 (d, *J* = 2.4 Hz, 1H), 10.4 (s, 1H). MS (ESI): [M + 1]⁺ = 285.2.

O-2-Acetyl-4-nitro-5-methoxyphenyl-*N,N*-dimethylcarbamothioate (5d). Using procedure A, the crude product was purified by crystallization from petroleum ether to give the product **5d** as a yellow solid; yield 83%; mp 122–123 °C. ¹H NMR (CDCl₃) δ: 2.60 (s, 3H), 3.06 (s, 3H), 3.14 (s, 3H), 4.03 (s, 3H), 7.53 (s, 1H), 8.27 (s, 1H). MS (ESI): [M + 1]⁺ = 299.2.

O-2-Acetyl-4-nitro-6-methoxyphenyl-*N,N*-dimethylcarbamothioate (5e). Using procedure A, the crude product was purified by crystallization from petroleum ether to give the product **5e** as a yellow solid; yield 88%; mp 101–103 °C. ¹H NMR (CDCl₃) δ: 2.60 (s, 3H), 3.42 (s, 3H), 3.45 (s, 3H), 3.94 (s, 3H), 7.92 (d, *J* = 2.4 Hz, 1H), 8.27 (d, *J* = 2.4 Hz, 1H). MS (ESI): [M + 1]⁺ = 299.3.

General Procedure B for the Preparation of Compounds 6a–e. The *N,N*-dimethylcarbamothioates **5a–e** (5 mmol) were dissolved in toluene (30 mL), and the mixtures were refluxed for 12 h. The solvent was evaporated in vacuo, and the residues were purified by column chromatography (petroleum ether–ethyl acetate as eluent) or by crystallization from petroleum ether.

S-2-Formyl-4-nitrophenyl-*N,N*-dimethylcarbamothioate (6a). Using general procedure B, the product **6a** was obtained by crystallization from petroleum ether as a yellow solid; 91% yield; mp 81–83 °C. ¹H NMR (CDCl₃) δ: 3.06 (s, 3H), 3.19 (s, 3H), 7.76 (d, *J*

= 8.4 Hz, 1H), 8.36 (dd, *J* = 8.4 and 2.4 Hz, 1H), 8.82 (d; *J* = 2.8 Hz, 1H), 10.3 (s, 1H). MS (ESI): [M + 1]⁺ = 255.0.

S-2-Acetyl-4-nitrophenyl-*N,N*-dimethylcarbamothioate (6b). Following general procedure B, the product **6b** purified by crystallization from petroleum ether was obtained as a red solid; 89% yield; mp 105–107 °C. ¹H NMR (CDCl₃) δ: 2.66 (s, 3H), 3.04 (s, 3H), 3.13 (s, 3H), 7.78 (d, *J* = 8.6 Hz, 1H), 8.27 (dd, *J* = 8.6 and 2.4 Hz, 1H), 8.44 (d, *J* = 2.4 Hz, 1H). MS (ESI): [M + 1]⁺ = 269.2.

S-2-Formyl-4-nitro-6-methoxyphenyl-*N,N*-dimethylcarbamothioate (6c). Using general procedure B, the product **6c** was obtained by crystallization from petroleum ether as a yellow solid; 95% yield; mp 168–170 °C. ¹H NMR (CDCl₃) δ: 3.03 (bs, 3H), 3.23 (bs, 3H), 4.02 (s, 3H), 7.94 (d, *J* = 2.6 Hz, 1H), 8.44 (d, *J* = 2.6 Hz, 1H), 10.4 (s, 1H). MS (ESI): [M + 1]⁺ = 285.3.

S-2-Acetyl-4-nitro-5-methoxyphenyl-*N,N*-dimethylcarbamothioate (6d). Using general procedure B, compound **6d** purified by column chromatography (40% ethyl acetate in petroleum ether) was obtained as a brown solid; 46% yield; mp 123–125 °C. ¹H NMR (CDCl₃) δ: 2.62 (s, 3H), 3.05 (s, 3H), 3.14 (s, 3H), 4.03 (s, 3H), 7.53 (s, 1H), 8.27 (s, 1H). MS (ESI): [M + 1]⁺ = 299.2.

S-2-Acetyl-4-nitro-6-methoxyphenyl-*N,N*-dimethylcarbamothioate (6e). Using general procedure B, compound **6e** purified by column chromatography (30% ethyl acetate in petroleum ether) was obtained as a yellow solid; 78% yield; mp 192–194 °C. ¹H NMR (CDCl₃) δ: 2.60 (s, 3H), 3.00 (s, 3H), 3.15 (s, 3H), 3.98 (s, 3H), 7.81 (d, *J* = 2.2 Hz, 1H), 7.93 (d, *J* = 2.2 Hz, 1H). MS (ESI): [M + 1]⁺ = 299.2.

General Procedure C for the Preparation of Compounds 7a–e.

The *S*-aryl compounds **6a–e** (1 mmol) were dissolved in MeOH (8 mL). A 3 N aqueous solution of NaOH (4 mL) was added, and the reaction mixtures were refluxed for 5 h. Upon completion, the mixtures were cooled to 25 °C and acidified to pH 3 by the addition of 10% aqueous HCl. The resulting mixtures were extracted with CH₂Cl₂ (3 × 10 mL), and the combined organic extracts were washed with brine, dried over Na₂SO₄, and evaporated to dryness under reduced pressure. The residues were purified by column chromatography on silica gel or by crystallization from petroleum ether.

2-Mercapto-5-nitrobenzaldehyde (7a). Using general procedure C, the residue was crystallized from petroleum ether to provide **7a** as a yellow solid; yield 92%; mp 147–149 °C. ¹H NMR (CDCl₃) δ: 6.12 (s, 1H), 7.52 (d, *J* = 8.6 Hz, 1H), 8.22 (dd, *J* = 8.6 and 2.4 Hz, 1H), 8.62 (d, *J* = 2.4 Hz, 1H), 10.1 (br s, 1H). MS (ESI): [M + 1]⁺ = 184.2.

1-(2-Mercapto-5-nitrophenyl)ethanone (7b). Using general procedure C, the crude residue was crystallized from petroleum ether to provide **7b** as a red solid; yield 85%; mp 93–95 °C. ¹H NMR (CDCl₃) δ: 2.73 (s, 3H), 5.01 (s, 1H), 7.44 (d, *J* = 8.6 Hz, 1H), 8.14 (dd, *J* = 8.6 and 2.6 Hz, 1H), 8.75 (d, *J* = 2.6 Hz, 1H). MS (ESI): [M + Na]⁺ = 209.1.

2-Mercapto-3-methoxy-5-nitrobenzaldehyde (7c). Using general procedure C, the crude residue was crystallized from petroleum ether to provide **7c** as a yellow solid; yield 90%; mp 101–103 °C. ¹H NMR (CDCl₃) δ: 4.09 (s, 3H), 6.10 (s, 1H), 7.86 (d, *J* = 2.4 Hz, 1H), 8.32 (d, 1H, *J* = 2.4 Hz), 10.1 (br s, 1H). MS (ESI): [M + 1]⁺ = 214.1.

1-(2-Mercapto-4-methoxy-5-nitrophenyl)ethanone (7d). Using general procedure C, the product **7d**, purified by column chromatography on silica gel (30% ethyl acetate in petroleum ether), was obtained as a yellow solid; yield 68%; mp 101–103 °C. ¹H NMR (CDCl₃) δ: 2.65 (s, 3H), 4.03 (s, 3H), 5.82 (bs, 1H), 6.92 (s, 1H), 8.54 (s, 1H). MS (ESI): [M + 1]⁺ = 228.1.

1-(2-Mercapto-3-methoxy-5-nitrophenyl)ethanone (7e). Following general procedure C, the product **7e**, purified by column chromatography (40% ethyl acetate in petroleum ether), was obtained as a yellow solid; yield 73%; mp 143–145 °C. ¹H NMR (CDCl₃) δ: 2.71 (s, 3H), 4.08 (s, 3H), 5.64 (bs, 1H), 7.83 (d, *J* = 2.2 Hz, 1H), 8.43 (d, *J* = 2.2 Hz, 1H). MS (ESI): [M + 1]⁺ = 228.2.

General Procedure D for the Preparation of Derivatives 8a–e.

To a solution of the substituted 2-mercaptobenzaldehyde **7a** or **7c** or 2-mercaptoacetophenone **7b**, **7d**, or **7e** (1 mmol) in acetone (15 mL) was added 2-bromo-1-(3,4,5-trimethoxyphenyl)ethanone (289 mg, 1 mmol) and anhydrous K₂CO₃ (276 mg, 2 mmol). The resulting

mixture was maintained at reflux for 18 h. After this time, acetone was removed by evaporation, and the residue was taken up in a CH₂Cl₂ (15 mL) and water (5 mL) mixture. The organic layer was washed with brine, dried over Na₂SO₄, and concentrated to dryness under reduced pressure. The crude residue was purified by flash column chromatography or by crystallization from petroleum ether.

(5-Nitrobenzo[b]thiophen-2-yl)(3,4,5-trimethoxyphenyl)methanone (8a). Using general procedure D, the crude product was purified by crystallization from petroleum ether to give **8a** as a brown solid; yield 81%; mp 185–187 °C. ¹H NMR (CDCl₃) δ: 3.92 (s, 6H), 3.96 (s, 3H), 7.18 (s, 2H), 7.20 (s, 1H), 8.03 (d, *J* = 8.6 Hz, 1H), 8.36 (dd, *J* = 8.6 and 1.8 Hz, 1H), 8.84 (d, *J* = 1.8 Hz, 1H). MS (ESI): [*M* + 1] = 374.2.

(3,4,5-Trimethoxyphenyl)(3-methyl-5-nitrobenzo[b]thiophen-2-yl)methanone (8b). Using general procedure D, the crude residue was purified by crystallization from petroleum ether to give **8b** as a brown solid; yield 53%; mp 120–122 °C. ¹H NMR (CDCl₃) δ: 2.64 (s, 3H), 3.92 (s, 6H), 3.94 (s, 3H), 7.18 (s, 2H), 8.00 (d, *J* = 8.6 Hz, 1H), 8.34 (dd, *J* = 8.6 and 2.0 Hz, 1H), 8.84 (s, 1H). MS (ESI): [*M* + 1] = 388.1.

(7-Methoxy-5-nitrobenzo[b]thiophen-2-yl)(3,4,5-trimethoxyphenyl)methanone (8c). Using general procedure D, the crude product purified by crystallization from petroleum ether furnished **8c** as a brown solid; yield 95%; mp 209–211 °C. ¹H NMR (CDCl₃) δ: 3.92 (s, 6H), 3.93 (s, 3H), 4.12 (s, 3H), 7.18 (s, 2H), 7.74 (s, 1H), 8.00 (s, 1H), 8.44 (s, 1H). MS (ESI): [*M* + 1] = 404.2.

(3-Methyl-6-methoxy-5-nitrobenzo[b]thiophen-2-yl)(3,4,5-trimethoxyphenyl)methanone (8d). Using general procedure D, the crude residue purified by crystallization from petroleum ether yielded **8d** as a brown solid; yield 86%; mp 198–200 °C. ¹H NMR (CDCl₃) δ: 2.57 (s, 3H), 3.90 (s, 3H), 3.92 (s, 3H), 3.96 (s, 3H), 4.05 (s, 3H), 7.15 (s, 2H), 7.46 (s, 1H), 8.34 (s, 1H). MS (ESI): [*M* + 1] = 418.1.

(3-Methyl-7-methoxy-5-nitrobenzo[b]thiophen-2-yl)(3,4,5-trimethoxyphenyl)methanone (8e). Using general procedure D, the crude residue purified by crystallization from petroleum ether furnished **8e** as a white solid; yield 80%; mp 166–168 °C. ¹H NMR (CDCl₃) δ: 2.63 (s, 3H), 3.89 (s, 6H), 3.93 (s, 3H), 4.10 (s, 3H), 7.18 (s, 2H), 7.72 (d, *J* = 1.8 Hz, 1H), 8.42 (d, *J* = 1.8 Hz, 1H). MS (ESI): [*M* + 1] = 418.1.

Preparation of (7-Methoxy-5-nitrobenzo[b]thiophen-2-yl)(4,5-dimethoxyphenyl)methanone (8f). Following general procedure D, using 2-mercaptobenzaldehyde **7c** and 2-bromo-1-(4,5-dimethoxyphenyl)ethanone as reagents, the residue was chromatographed with 30% EtOAc in petroleum ether to give **8f** as a yellow solid; yield 73%; mp 167–168 °C. ¹H NMR (CDCl₃) δ: 3.97 (s, 3H), 3.99 (s, 3H), 4.12 (s, 3H), 6.36 (d, *J* = 8.2 Hz, 1H), 7.53 (d, *J* = 8.2 Hz, 1H), 7.64 (d, *J* = 8.2 Hz, 1H), 7.71 (d, *J* = 2.0 Hz, 1H), 7.87 (s, 1H), 8.44 (s, 1H). MS (ESI): [*M* + 1] = 374.2.

Preparation of (7-Methoxy-5-nitrobenzo[b]thiophen-2-yl)(4-methoxyphenyl)methanone (8g). Following general procedure D, using 2-mercaptobenzaldehyde **7c** and 2-bromo-1-(4-methoxyphenyl)ethanone as reagents, the residue was chromatographed with 30% EtOAc in petroleum ether to give **8g** as a yellow solid; yield 68%; mp 152–154 °C. ¹H NMR (CDCl₃) δ: 3.92 (s, 3H), 4.12 (s, 3H), 7.01 (d, *J* = 8.8 Hz, 2H), 7.72 (s, 1H), 7.94 (d, *J* = 8.8 Hz, 2H), 7.98 (s, 1H), 8.44 (d, *J* = 1.8 Hz, 1H). MS (ESI): [*M* + 1] = 344.1.

General Procedure E for the Synthesis of Compounds 3a–e and 3p–q. To a suspension of nitro derivatives **8a–g** (1 mmol) in absolute ethanol (10 mL) was added SnCl₂·2H₂O (5 mmol), and the stirring mixtures were refluxed for 1 h. After this time, the reactions were allowed to cool to ambient temperature, treated with 15 mL of water, and neutralized with NaHCO₃. The mixtures were extracted with EtOAc (3 × 20 mL), and the organic layers were washed with water and brine, dried over Na₂SO₄, and concentrated under reduced pressure to residues that were purified by flash column chromatography to furnish **3a–e** and **3p–q**.

(5-Aminobenzo[b]thiophen-2-yl)(3,4,5-trimethoxyphenyl)methanone (3a). Using general procedure E, the residue was chromatographed with 30% EtOAc in petroleum ether to give **3a** as a yellow solid; yield 58%; mp 65–67 °C. ¹H NMR (CDCl₃) δ: 3.68 (bs, 2H), 3.91 (s, 6H), 3.94 (s, 3H), 6.91 (dd, *J* = 8.8 and 2.4 Hz, 1H),

7.12 (d, *J* = 2.4 Hz, 1H), 7.19 (s, 2H), 7.65 (d, *J* = 8.6 Hz, 1H), 7.72 (s, 1H). MS (ESI): [*M* + 1] = 344.1. Anal. (C₁₈H₁₇NO₄S) C, H, N.

(3,4,5-Trimethoxyphenyl)(3-methyl-5-aminobenzo[b]thiophen-2-yl)methanone (3b). Using general procedure E, the crude residue purified by column chromatography (30% EtOAc in petroleum ether) furnished **3b** as a brown solid; yield 67%; mp 165–167 °C. ¹H NMR (CDCl₃) δ: 2.53 (s, 3H), 3.82 (bs, 2H), 3.89 (s, 6H), 3.92 (s, 3H), 6.96 (dd, *J* = 8.8 and 2.4 Hz, 1H), 7.11 (d, *J* = 2.4 Hz, 1H), 7.19 (s, 2H), 7.62 (d, *J* = 8.6 Hz, 1H). MS (ESI): [*M*]⁺ = 358.3. Anal. (C₁₉H₁₉NO₄S) C, H, N.

(7-Methoxy-5-aminobenzo[b]thiophen-2-yl)(3,4,5-trimethoxyphenyl)methanone (3c). Using general procedure E, the crude residue purified by column chromatography (40% EtOAc in petroleum ether) gave **3c** as a yellow solid; yield 71%; mp 176–178 °C. ¹H NMR (CDCl₃) δ: 3.86 (bs, 2H), 3.91 (s, 6H), 3.93 (s, 3H), 3.96 (s, 3H), 6.36 (d, *J* = 2.0 Hz, 1H), 6.75 (d, *J* = 2.0 Hz, 1H), 7.17 (s, 2H), 7.71 (s, 1H). MS (ESI): [*M*]⁺ = 374.2. Anal. (C₁₉H₁₉NO₅S) C, H, N.

(3-Methyl-6-methoxy-5-aminobenzo[b]thiophen-2-yl)(3,4,5-trimethoxyphenyl)methanone (3d). Using general procedure E, the residue purified by column chromatography (50% EtOAc in petroleum ether) furnished **3d** as a yellow solid; yield 60%; mp 193–195 °C. ¹H NMR (CDCl₃) δ: 2.54 (s, 3H), 3.80 (bs, 2H), 3.89 (s, 3H), 3.94 (s, 6H), 3.96 (s, 3H), 7.11 (s, 1H), 7.16 (s, 1H), 7.17 (s, 2H). MS (ESI): [*M*]⁺ = 388.2. Anal. (C₂₀H₂₁NO₅S) C, H, N.

(3-Methyl-7-methoxy-5-aminobenzo[b]thiophen-2-yl)(3,4,5-trimethoxyphenyl)methanone (3e). Using general procedure E, the crude residue was purified by crystallization from petroleum ether to give **3e** as a yellow solid; yield 82%; mp 193–195 °C. ¹H NMR (CDCl₃) δ: 2.52 (s, 3H), 3.84 (bs, 2H), 3.89 (s, 6H), 3.93 (s, 3H), 3.95 (s, 3H), 6.36 (d, *J* = 1.8 Hz, 1H), 6.72 (d, *J* = 1.8 Hz, 1H), 7.19 (s, 2H). MS (ESI): [*M*]⁺ = 388.3. Anal. (C₂₀H₂₁NO₅S) C, H, N.

(7-Methoxy-5-aminobenzo[b]thiophen-2-yl)(4,5-dimethoxyphenyl)methanone (3p). Using general procedure E, the residue chromatographed with 40% EtOAc in petroleum ether gave **3p** as a yellow solid; yield 73%; mp 156–158 °C. ¹H NMR (CDCl₃) δ: 3.78 (bs, 2H), 3.95 (s, 3H), 3.96 (s, 3H), 3.98 (s, 3H), 6.34 (d, *J* = 1.8 Hz, 1H), 6.74 (d, *J* = 1.8 Hz, 1H), 6.92 (d, *J* = 8.2 Hz, 1H), 7.49 (d, *J* = 2.0 Hz, 1H), 7.59 (dd, *J* = 8.2 and 1.8 Hz, 1H), 7.68 (s, 1H). MS (ESI): [*M*]⁺ = 344.2. Anal. (C₁₈H₁₇NO₅S) C, H, N.

(7-Methoxy-5-aminobenzo[b]thiophen-2-yl)(4-methoxyphenyl)methanone (3q). Following general procedure E, the residue chromatographed with 40% EtOAc in petroleum ether furnished **3q** as a yellow solid; yield 67%; mp 190–192 °C. ¹H NMR (CDCl₃) δ: 3.78 (bs, 2H), 3.90 (s, 3H), 3.96 (s, 3H), 6.34 (d, *J* = 1.4 Hz, 1H), 6.73 (d, *J* = 1.4 Hz, 1H), 6.98 (d, *J* = 8.6 Hz, 2H), 7.65 (s, 1H), 7.92 (d, *J* = 8.6 Hz, 2H). MS (ESI): [*M*]⁺ = 314.1. Anal. (C₁₇H₁₅NO₃S) C, H, N.

Synthesis of (5-(Methylamino)-7-methoxybenzo[b]thiophen-2-yl)(3,4,5-trimethoxyphenyl)methanone (3f) and (5-(Dimethylamino)-7-methoxybenzo[b]thiophen-2-yl)(3,4,5-trimethoxyphenyl)methanone (3g). K₂CO₃ (83 mg, 0.6 mmol) was added to a mixture of CH₃I (0.058 mL, 0.9 mmol) and **3c** (112 mg, 0.3 mmol) in 4 mL of anhydrous DMF. The mixture was stirred at 40 °C for 48 h. After this period, CH₃I (0.058 mL, 0.9 mmol) was added, and after 24 h, the reaction mixture was diluted with cold water (1 mL) and extracted with CH₂Cl₂ (3 × 5 mL). The organic extracts were combined, washed with water (2 mL) and brine, dried over Na₂SO₄, and concentrated in vacuo. The crude residue was purified by flash column chromatography using ethyl acetate–petroleum ether 4:6 (v:v) as eluent to afford **3f** and **3g**.

(5-(Methylamino)-7-methoxybenzo[b]thiophen-2-yl)(3,4,5-trimethoxyphenyl)methanone (3f). Yellow oil; yield 22%. ¹H NMR (CDCl₃) δ: 2.89 (s, 3H), 3.91 (s, 3H), 3.93 (s, 6H), 3.96 (s, 3H), 4.04 (bs, 1H), 6.30 (s, 1H), 6.63 (s, 1H), 7.19 (s, 2H), 7.76 (s, 1H). MS (ESI): [*M* + 1]⁺ = 388.2. Anal. (C₂₀H₂₁NO₅S) C, H, N.

(5-(Dimethylamino)-7-methoxybenzo[b]thiophen-2-yl)(3,4,5-trimethoxyphenyl)methanone (3g). Brown oil; 41% yield. ¹H NMR (CDCl₃) δ: 3.00 (s, 6H), 3.91 (s, 3H), 3.94 (s, 6H), 3.99 (s, 3H), 6.50 (s, 1H), 6.72 (s, 1H), 7.18 (s, 2H), 7.77 (s, 1H). MS (ESI): [*M* + 1]⁺ = 402.4. Anal. (C₂₁H₂₃NO₅S) C, H, N.

***N*-[7-Methoxy-2-(3,4,5-trimethoxybenzoyl)-1-benzo[*b*]thien-5-yl]acetamide (3h).** To a solution of 3c (373 mg, 1 mmol) and pyridine (0.24 mL, 3 mmol) in dry CH₂Cl₂ (5 mL), acetyl chloride (0.21 mL, 3 mmol) was added at 0 °C. The reaction mixture was stirred for 2 h at room temperature, diluted with CH₂Cl₂ (5 mL), washed with water (4 mL), dried over Na₂SO₄, and concentrated in vacuo. The crude residue was purified by column chromatography (20% petroleum ether in ethyl acetate) to give 3h as a yellow solid; yield 69%; mp 141–143 °C. ¹H NMR (CDCl₃) δ: 2.17 (s, 3H), 3.92 (s, 6H), 3.96 (s, 3H), 4.01 (s, 3H), 7.12 (bs, 1H), 7.18 (s, 2H), 7.27 (s, 1H), 7.69 (s, 1H), 7.84 (s, 1H). MS (ESI): [M]⁺ = 416.5. Anal. (C₂₁H₂₁NO₆S) C, H, N.

2-Chloro-*N*-[7-methoxy-2-(3,4,5-trimethoxybenzoyl)-1-benzo[*b*]thien-5-yl]acetamide (3k). To a solution of 3c (373 mg, 1 mmol) and pyridine (0.24 mL, 3 mmol) in dry CH₂Cl₂ (5 mL), chloroacetyl chloride (0.24 mL, 3 mmol) was added at 0 °C. The reaction mixture was stirred for 1 h at room temperature, diluted with CH₂Cl₂ (10 mL), washed with water (5 mL), dried over Na₂SO₄, and concentrated in vacuo. The crude residue was purified by column chromatography (30% ethyl acetate in petroleum ether) to furnish 3k as a yellow solid; yield 96%; mp 81–83 °C. ¹H NMR (CDCl₃) δ: 3.92 (s, 6H), 3.96 (s, 3H), 4.04 (s, 3H), 4.24 (s, 2H), 7.10 (d, *J* = 1.6 Hz, 1H), 7.19 (s, 2H), 7.84 (d, *J* = 1.6 Hz, 1H), 7.86 (s, 1H), 8.32 (bs, 1H). MS (ESI): [M + 1]⁺ = 450.4. Anal. (C₂₁H₂₀ClNO₆S) C, H, N.

General Procedure F for the Preparation of Compounds 3i and 3l. To a solution of aminobenzo[*b*]thiophene 3a or 3c (1 mmol) and pyridine (0.24 mL, 3 mmol) in dry CH₂Cl₂ (5 mL), bromoacetyl chloride (0.25 mL, 3 mmol) was added at 0 °C. After 3 h at the same temperature, the reaction mixture was diluted with CH₂Cl₂ (5 mL), washed with water (5 mL), and dried (Na₂SO₄). CH₂Cl₂ was concentrated under reduced pressure and the crude residue purified by flash column chromatography.

2-Bromo-*N*-[2-(3,4,5-trimethoxybenzoyl)-1-benzo[*b*]thien-5-yl]acetamide (3i). Using general procedure F, the crude residue purified by flash chromatography (60% EtOAc in petroleum ether) furnished 3i as a brown solid; yield 82%; mp 164–166 °C. ¹H NMR (CDCl₃) δ: 3.92 (s, 6H), 3.96 (s, 3H), 4.07 (s, 2H), 7.18 (s, 2H), 7.42 (dd, *J* = 8.6 and 2.2 Hz, 1H), 7.83 (s, 1H), 7.88 (t, *J* = 4.4 Hz, 1H), 8.28 (bs, 1H), 8.34 (d, *J* = 2.2 Hz, 1H). MS (ESI): [M]⁺ = 464.4, [M + 2]⁺ = 466.4. Anal. (C₂₀H₁₈BrNO₅S) C, H, N.

2-Bromo-*N*-[7-methoxy-2-(3,4,5-trimethoxybenzoyl)-1-benzo[*b*]thien-5-yl]acetamide (3l). Using general procedure F, the crude residue purified by flash chromatography (50% EtOAc in petroleum ether) furnished 3l as a brown solid; yield 81%; mp 183–185 °C. ¹H NMR (CDCl₃) δ: 3.92 (s, 6H), 3.95 (s, 3H), 4.03 (s, 3H), 4.07 (s, 2H), 7.10 (d, *J* = 1.6 Hz, 1H), 7.18 (s, 2H), 7.74 (d, *J* = 1.6 Hz, 1H), 7.85 (s, 1H), 8.26 (bs, 1H). MS (ESI): [M]⁺ = 494.4, [M + 2]⁺ = 496.4. Anal. (C₂₁H₂₀BrNO₆S) C, H, N.

General Procedure G for the Preparation of Compounds 3j and 3m. A mixture of bromoacetamide derivatives 3i or 3l (1 mmol) and NaI (1.5 g, 10 mmol) in *N,N*-dimethylacetamide (5 mL) was stirred at ambient temperature for 18 h. DMA was evaporated under reduced pressure, followed by addition of CH₂Cl₂ (15 mL) and a solution of Na₂S₂O₃ (10%, 5 mL). The organic layer was washed with water (5 mL) and brine (5 mL) and dried over Na₂SO₄. After evaporation of the solvent, the residue was purified by chromatography on silica gel.

2-Iodo-*N*-[2-(3,4,5-trimethoxybenzoyl)-1-benzo[*b*]thien-5-yl]acetamide (3j). Using general procedure G, the residue purified by flash chromatography (50% ethyl acetate in petroleum ether) yielded 3j as a brown solid; 86% yield; mp 172–174 °C. ¹H NMR (CDCl₃) δ: 3.89 (s, 6H), 3.92 (s, 3H), 3.96 (s, 2H), 7.18 (s, 2H), 7.40 (dd, *J* = 8.6 and 2.0 Hz, 1H), 7.87 (t, *J* = 4.4 Hz, 1H), 7.88 (s, 1H), 8.29 (bs, 1H), 8.34 (d, *J* = 2.0 Hz, 1H). MS (ESI): [M]⁺ = 511.3. Anal. (C₂₀H₁₈IINO₅S) C, H, N.

2-Iodo-*N*-[7-methoxy-2-(3,4,5-trimethoxybenzoyl)-1-benzo[*b*]thien-5-yl]acetamide (3m). Using general procedure G, the residue purified by flash chromatography (50% ethyl acetate in petroleum ether 1:1) gave 3m as a brown solid; yield 84%; mp 200–202 °C. ¹H NMR (CDCl₃) δ: 3.89 (s, 6H), 3.91 (s, 3H), 3.95 (s, 3H), 4.01 (s,

2H), 7.11 (s, 1H), 7.18 (s, 2H), 7.69 (s, 1H), 7.83 (s, 1H), 7.88 (bs, 1H). MS (ESI): [M]⁺ = 541.3. Anal. (C₂₁H₂₀IINO₆S) C, H, N.

General Procedure H for the Synthesis of Compounds 3n and 3o. To an ice-cooled solution of aminobenzo[*b*]thiophene 3a or 3c (1 mmol) in dry DMF (5 mL) were added EDCI (383 mg, 2 mmol) and HOBt (270 mg, 2 mmol), followed by α-bromoacrylic acid (2 mmol, 306 mg). The reaction solution was stirred at ambient temperature for 18 h and evaporated under reduced pressure. The crude material was dissolved with a mixture of CH₂Cl₂ (15 mL) and water (5 mL), and the organic phase was washed with brine (5 mL), dried over Na₂SO₄, and evaporated to dryness in vacuo. The resulting crude residue was purified by column chromatography on silica gel.

2-Bromo-*N*-[2-(3,4,5-trimethoxybenzoyl)-1-benzo[*b*]thien-5-yl]acrylamide (3n). Using general procedure H, the crude residue, purified by flash chromatography by eluting with a mixture of EtOAc–petroleum ether 1:1 (v:v), furnished 3n as a brown solid; yield 71%; mp 150–151 °C. ¹H NMR (CDCl₃) δ: 3.91 (s, 6H), 3.94 (s, 3H), 6.16 (d, *J* = 1.6 Hz, 1H), 7.12 (d, *J* = 1.6 Hz, 1H), 7.14 (s, 1H), 7.18 (s, 2H), 7.42 (dd, *J* = 8.8 and 1.8 Hz, 1H), 7.87 (d, *J* = 8.8 Hz, 1H), 8.42 (d, *J* = 1.8 Hz, 1H), 8.54 (bs, 1H). MS (ESI): [M]⁺ = 476.4, [M + 2]⁺ = 478.4. Anal. (C₂₁H₁₈BrNO₅S) C, H, N.

2-Bromo-*N*-[7-methoxy-2-(3,4,5-trimethoxybenzoyl)-1-benzo[*b*]thien-5-yl]acrylamide (3o). Using general procedure H, the crude residue, purified by flash chromatography by eluting with a solution of EtOAc–petroleum ether 1:1 (v:v), furnished 3o as a yellow solid; yield 62%; mp 165–167 °C. ¹H NMR (CDCl₃) δ: 3.92 (s, 6H), 3.95 (s, 3H), 4.03 (s, 3H), 6.17 (d, *J* = 1.6 Hz, 1H), 7.15 (d, *J* = 1.6 Hz, 1H), 7.16 (s, 1H), 7.18 (s, 2H), 7.73 (s, 1H), 7.85 (s, 1H), 8.49 (bs, 1H). MS (ESI): [M]⁺ = 506.4, [M + 2]⁺ = 508.4. Anal. (C₂₂H₂₀BrNO₆S) C, H, N.

Biology. Antiproliferative Assays. Murine leukemia (L1210), murine mammary carcinoma (FM3A), human T-lymphoblastoid (Molt/4 and CEM), and human cervix carcinoma (HeLa) cells were suspended at (3–5) × 10⁵ cells/mL of culture medium, and 100 μL of a cell suspension was added to 100 μL of an appropriate dilution of the test compounds in wells of 96-well microtiter plates. After incubation at 37 °C for 48 h, cell number was determined using a Coulter counter as previously described.⁴¹ The IC₅₀ was defined as the concentration of compound that inhibited cell proliferation by 50%.

PBL from healthy donors were obtained by separation on Lymphoprep (Fresenius KABI Norge AS) gradient. After extensive washing, cells were resuspended (1.0 × cells/mL) in RPMI-1640 with 10% fetal bovine serum and incubated overnight in a 96-well tissue culture microtiter plate. For cytotoxicity evaluations of proliferating PBL cultures, nonadherent cells were resuspended at 5 × 10⁵ cells/mL in growth medium containing 2.5 μg/mL PHA (Irvine Scientific). Varying amounts of compounds being evaluated were added to the cells, and the MTT assay⁴² was used to assess viability after a 72 h treatment.

HUVECs were obtained from human umbilical veins.⁴³ The adherent cell population was grown in M200 medium containing Low Serum Growth Supplement (contains fetal bovine serum (FBS), bFGF, heparin, hEGF, gentamycin, hydrocortisone and amphotericin B), which was purchased from Life Technologies, Monza, Italy. When the cells grew to confluence, they were detached from the plate with a solution containing EDTA and trypsin. Only HUVECs from the first to the sixth passage were used in viability experiments. In these experiments, varying concentrations of the compounds of interest were added, with ability again determined after a 72 h treatment by MTT assay.⁴²

Tubulin Polymerization Assay. Bovine brain tubulin (10 μM) in 0.8 M glutamate was preincubated with varying concentrations of drug for 15 min at 30 °C, and then the samples were cooled on ice. After addition of 0.4 mM GTP, the reaction mixtures were pipetted into 0 °C cuvettes in temperature controlled recording spectrophotometers. The effect of each agent on tubulin polymerization was followed turbidimetrically at 350 nm for 20 min at 30 °C. The IC₅₀ was defined as the compound concentration that inhibited tubulin polymerization by 50%. Complete experimental details were previously described.²³

[³H]Colchicine Binding. Each reaction mixture contained 1.0 μM tubulin, 5.0 μM [³H]colchicine, and 1.0 or 5.0 μM tested compound. The mixtures were incubated for 10 min at 37 °C. Full experimental details were described previously.²⁵

Molecular Modeling. Molecular docking simulations were carried out on a MacPro dual 2.66 GHz Xeon running Ubuntu 12.04, using the tubulin structure reported by A. Dorleans et al. (PDB code: 3HKC).⁴⁴ Molecular Operating Environment (MOE) was used to prepare the protein structure by adding the hydrogen atoms using the Protonate3D function.⁴⁵ MOE was also used to build the ligand structures, which were minimized using the MMFF94x force field until a RMSD gradient of 0.05 kcal mol⁻¹ Å⁻¹ was reached. The software package PLANTS was then used to perform the docking simulations.⁴⁶

Flow Cytometric Analysis of Cell Cycle Distribution. HeLa cells (5 × 10⁵), treated with varying amounts of the desired agents, were grown for 24 or 48 h. At these times, the cells were harvested by centrifugation and fixed with 70% (v/v) ethanol that had been chilled to 0 °C. The cells were suspended in a solution that contained RNase and 0.1% (v/v) Triton X-100. Their DNA was then stained with PI. Each sample was processed on a Beckman-Coulter Cytomic FC500 flow cytometer. DNA content was analyzed in a histogram format using MultiCycle for Windows from Phoenix Flow Systems.

Annexin-V Assay. The appearance of phosphatidylserine on the surface of apoptotic cells was measured with annexin-V conjugated to fluorescein isothiocyanate (FITC), and DNA in the cells was measured with PI. The flow cytometer described above was also used in these experiments. Staining of the cells prior to analysis was performed as instructed by Roche Diagnostics, the manufacturer of Annexin-V Fluos. The excitation wavelength was 488 nm, and emission at 525 nm was used to quantitate the FITC and at 585 nm to quantitate the PI.

Assessment of Mitochondrial Changes. The mitochondrial membrane potential was measured with the fluorescent probe JC-1 (Molecular Probes), as described.⁴² The generation of ROS was measured by flow cytometry using H₂DCFDA (Molecular Probes), as previously described.⁴²

Western Blot Analysis. Aliquots of HeLa cell cultures, both control and containing the desired compounds at the indicated concentration, were removed at time points as indicated. The cells were collected by centrifugation and washed twice with phosphate-buffered saline chilled to 0 °C. The cells were then suspended in a lysis buffer at 0 °C for 30 min. The resulting suspensions were clarified by centrifugation (15000g, 4 °C, 10 min) and the protein concentrations of the supernatants determined with the BCA protein kit (Pierce, Italy). Protein aliquots of 20 μg were subjected to sodium dodecyl sulfate–polyacrylamide gel electrophoresis using 7.5–15% gradient polyacrylamide gels. Proteins were then electroblotted to PVDF Hybond-p membranes from GE Healthcare. The membranes were then treated with ECL advance blocking agent from GE Healthcare, using a rotary shaker at 4 °C, as instructed by the manufacturer. Membranes were next incubated for 2 h at room temperature with a variety of primary antibodies from Cell Signaling, Alexis, Upstate, and Sigma-Aldrich, as indicated in the individual experiments. Finally, membranes were incubated with peroxidase-labeled secondary antibodies for 60 min. All membranes were visualized using ECL Advance (GE Healthcare) and exposed to Hyperfilm MP (GE Healthcare). To ensure equal protein loading, each membrane was stripped and reprobed with an anti-β-actin antibody.

Antitumor Activity in V. BALB/c-nu mice (age 4 weeks, sex female, weight 15–18 g) were purchased from the Shanghai (China) SLAC Laboratory Animal Co., Ltd. The mice were kept under specific pathogen-free conditions, with free access to food and water, in the Laboratory Animal Center of the Zhejiang University of Traditional Chinese Medicine. HNNG/HOS cells, derived from a human osteosarcoma, were grown into exponential phase. The cells were suspended in FBS-free MEM (10⁷ cells/mL), and 0.1 mL was injected into the hypodermis of the back of each mouse. When each of the xenografts was about 100 mm³ large, 12 mice were randomly placed in three groups: vehicle-treated control, CA-4P-treated (compound dissolved in isotonic saline), and 3c-treated (compound dissolved in 5% (v/v) DMSO in olive oil). Both compounds were given

intraperitoneally at 0.01 mL/g of weight of the mouse or a total dose of 50 mg/kg. Administration of vehicle or compound was once every 3 days for a total of four doses, with the first dose administered on day 0, the last on day 9. On day 18, all mice were euthanized. The formula $V = (L \times W^2)/W$ was used to calculate tumor volume, with V being volume, L being length, and W being width of the tumor nodules. L and W were measured using a vernier calliper. Approval of this study was obtained from the Institutional Animal Ethical Committee of the Second Affiliate Hospital, School of Medicine, Zhejiang University, PRC.

■ ASSOCIATED CONTENT

📄 Supporting Information

Proposed binding mode of compound 3c with colchicine in the β-tubulin binding site. This material is available free of charge via the Internet at <http://pubs.acs.org>.

■ AUTHOR INFORMATION

Corresponding Authors

*For R.R.: phone, 39-(0)532-455303; fax, 39-(0)532-455953; E-mail, rnr@unife.it.

*For P.G.B.: phone, 39-(0)532-455293; fax, 39-(0)532-455953; E-mail, pgb@unife.it.

*For G.V.: phone, 39-(0)49-8211451; fax, 39-(0)49-8211462; E-mail, giampietro.viola1@unipd.it.

Notes

The authors declare no competing financial interest.

■ ACKNOWLEDGMENTS

Jan Balzarini is funded by GOA (Krediet no. 10/14) of the KU Leuven. We gratefully acknowledge Alberto Casolari and Lizette van Berckelaer for their excellent technical assistance.

■ ABBREVIATIONS USED

CA-4, combretastatin A-4; CA-4P, combretastatin A-4 disodium phosphate; DABCO, 1,4-diazabicyclo[2,2,2]octane; DMF, *N,N'*-dimethylformamide; DMA, *N,N*-dimethylacetamide; EDCI, 1-ethyl-3-[3-(dimethylamino)propyl]-carbodiimide hydrochloride; SAR, structure–activity relationships; PI, propidium iodide; FITC, fluorescein isothiocyanate; JC-1, 5,5',6,6'-tetrachloro-1,1',3,3'-tetraethylbenzimidazolcarbocyanine; ROS, reactive oxygen species; H₂DCFDA, 2,7-dichlorodihydrofluorescein; PARP, poly-ADP-ribose polymerase

■ REFERENCES

- (1) Amos, L. A. Microtubule structure and its stabilisation. *Org. Biomol. Chem.* **2004**, *2*, 2153–2160.
- (2) Walczak, C. E. Microtubule dynamics and tubulin interacting proteins. *Curr. Opin. Cell. Biol.* **2000**, *12*, 52–56.
- (3) Downing, K. H.; Nogales, E. Tubulin structure: insights into microtubule properties and functions. *Curr. Opin. Struct. Biol.* **1998**, *8*, 785–791.
- (4) Dumontet, C.; Jordan, M. A. Microtubule-binding agents: a dynamic field of cancer therapeutics. *Nature Rev. Drug. Discovery* **2010**, *9*, 790–803.
- (5) Chen, S.-M.; Meng, L.-H.; Ding, J. New microtubule-inhibiting anticancer agents. *Expert Opin. Invest. Drugs* **2010**, *3*, 329–343.
- (6) Pasquier, E.; Kavallaris, M. Microtubules: a dynamic target in cancer therapy. *IUBMB Life* **2008**, *60*, 165–170.
- (7) Hamel, E. An overview of compounds that interact with tubulin and their effects on microtubule assembly. In *The Role of Microtubules in Cell Biology, Neurobiology and Oncology*; Fojo, T., Ed.; Human Press: Totowa, NJ, 2008; pp 1–19.

- (8) Carlson, R. O. New tubulin targeting agents currently in clinical development. *Expert Opin. Invest. Drugs* **2008**, *17*, 707–722.
- (9) Pettit, G. R.; Singh, S. B.; Hamel, E.; Lin, C. M.; Alberts, D. S.; Garcia-Kendall, D. Isolation and structure of the strong cell growth and tubulin inhibitor combretastatin A-4. *Experientia* **1989**, *45*, 209–211.
- (10) Lin, C. M.; Ho, H. H.; Pettit, G. R.; Hamel, E. Antimitotic natural products combretastatin A-4 and combretastatin A-2: studies on the mechanism of their inhibition of the binding of colchicine to tubulin. *Biochemistry* **1989**, *28*, 6984–6991.
- (11) Patterson, D. M.; Rustin, G. J. S. Combretastatin A-4 phosphate. *Drugs Future* **2007**, *32*, 1025–1032.
- (12) Petit, I.; Karajannis, M. A.; Vincent, L.; Young, L.; Butler, J.; Hopper, A. T.; Shido, K.; Steller, H.; Chaplin, D. J.; Feldman, E.; Rafi, S. The microtubule-targeting agent CA-4P regresses leukemic xenografts by disrupting interaction with vascular cells and mitochondrial-dependent cell death. *Blood* **2008**, *111*, 1951–1961.
- (13) Siemann, D. W.; Chaplin, D. J.; Walike, P. A. A review and update of the current status of the vasculature-disabling agent combretastatin-A4 phosphate (CA4P). *Expert Opin. Invest. Drugs* **2009**, *18*, 189–197.
- (14) Rustin, G. J.; Shreeves, G.; Nathan, P. D.; Gaya, A.; Ganesan, T. S.; Wang, D.; Boxall, J.; Poupard, L.; Chaplin, D. J.; Stratford, M. R. L.; Balkissoon, J.; Zweifel, M. A Phase Ib trial of CA4P (combretastatin A-4 phosphate), carboplatin, and paclitaxel in patients with advanced cancer. *Br. J. Cancer* **2010**, *102*, 1355–1360.
- (15) Romagnoli, R.; Baraldi, P. G.; Carrion, M. D.; Lopez-Cara, C.; Preti, D.; Fruttarolo, F.; Pavani, M. G.; Tabrizi, M. A.; Tolomeo, M.; Grimaudo, S.; Di Antonella, C.; Balzarini, J.; Hadfield, J. A.; Brancale, A.; Hamel, E. Synthesis and biological evaluation of 2- and 3-aminobenzo[b]thiophene derivatives as antimitotic agents and inhibitors of tubulin polymerization. *J. Med. Chem.* **2007**, *50*, 2273–2277.
- (16) Jiang, J.-D.; Roboz, J.; Weisz, I.; Deng, L.; Ma, L.; Holland, J. F.; Bekesi, J. G. Synthesis, anticancer and antimicrotubule activities of 3-(haloacetamido)-benzoylureas. *Anti-Cancer Drug Des.* **1998**, *13*, 735–747.
- (17) Song, D. Q.; Wang, Y.; Wu, L. Z.; Yang, P.; Wang, Y. M.; Gao, L. M.; Li, Y.; Qu, J. R.; Wang, Y. H.; Li, Y. H.; Du, N. N.; Han, Y. X.; Zhang, Z. P.; Jiang, J. D. Benzoylurea derivatives as a novel class of antimitotic agents: synthesis, anticancer activity and structure–activity relationships. *J. Med. Chem.* **2008**, *51*, 3094–3103.
- (18) Luduena, R. F.; Roach, M. C. Tubulin sulfhydryl groups as probes and targets for antimitotic and antimicrotubule agents. *Pharmacol. Ther.* **1991**, *49*, 133–152.
- (19) Hargreaves, A. J.; Glazier, A. P.; Flaskos, J.; Mullins, F. H.; Mcan, W. G. The disruption of brain microtubules in vitro by the phospholipase inhibitor *p*-bromophenacyl bromide. *Biochem. Pharmacol.* **1994**, *47*, 1137–1143.
- (20) Beria, I.; Baraldi, P. G.; Cozzi, P.; Caldarelli, M.; Geroni, C.; Marchini, S.; Mongelli, N.; Romagnoli, R. Cytotoxic α -halogenoacrylic derivatives of distamycin A and congeners. *J. Med. Chem.* **2004**, *47*, 2611–2623.
- (21) Compounds **4a–c** are commercially available. For the synthesis of **4d**, see: Banks, C. K.; Hamilton, C. S. Arsenated derivatives of mixed ketones. II. Arsenicals of peonol. *J. Am. Chem. Soc.* **1938**, *60*, 1370–1371. For the preparation of **4e**, see: Horton, W. J.; Spence, J. T. Hydrogen bromide cleavage of hindered 2'-methoxyacetophenones. *J. Am. Chem. Soc.* **1958**, *80*, 2453–2456.
- (22) For a review on the mechanism and application of Newman–Kwart rearrangement see: Lloyd-Jones, G. C.; Moseley, J. D.; Renny, J. S. Mechanism and application of the Newman–Kwart O–S rearrangement of O-aryl thiocarbamates. *Synthesis* **2008**, *5*, 661–689.
- (23) Hamel, E. Evaluation of antimitotic agents by quantitative comparisons of their effects on the polymerization of purified tubulin. *Cell Biochem. Biophys.* **2003**, *38*, 1–21.
- (24) Hiser, L.; Aggarwal, A.; Young, R.; Frankfurter, A.; Spano, A.; Correia, J. J.; Lobert, S. Comparison of β -tubulin mRNA and protein levels in 12 human cancer cell lines. *Cell Motil. Cytoskeleton* **2006**, *63*, 41–52.
- (25) Verdier-Pinard, P.; Lai, J.-Y.; Yoo, H.-D.; Yu, J.; Marquez, B.; Nagle, D. G.; Nambu, M.; White, J. D.; Falck, J. R.; Gerwick, W. H.; Day, B. W.; Hamel, E. Structure–activity analysis of the interaction of curacin A, the potent colchicine site antimitotic agent, with tubulin and effects of analogs on the growth of MCF-7 breast cancer cells. *Mol. Pharmacol.* **1998**, *53*, 62–67.
- (26) Massarotti, A.; Coluccia, A.; Silvestri, R.; Sorba, G.; Brancale, A. The tubulin colchicine domain: a molecular modeling perspective. *ChemMedChem* **2012**, *7*, 33–42.
- (27) Clarke, P. R.; Allan, L. A. Cell-cycle control in the face of damage—a matter of life or death. *Trends Cell Biol.* **2009**, *19*, 89–98.
- (28) Kiyokawa, H.; Ray, D. In vivo roles of Cdc25 phosphatases: biological insight into the anti-cancer therapeutic targets. *Anticancer Agents Med. Chem.* **2008**, *8*, 832–836.
- (29) Donzelli, M.; Draetta, G. F. Regulating mammalian checkpoints through cdc25 inactivation. *EMBO Rep.* **2003**, *4*, 671–677.
- (30) (a) Quignon, F.; Rozier, L.; Lachages, A. M.; Bieth, A.; Simili, M.; Debatisse, M. Sustained mitotic block elicits DNA breaks: one step alteration of ploidy and chromosome integrity in mammalian cells. *Oncogene* **2007**, *26*, 165–172. (b) Ganem, N. J.; Pellman, D. Linking abnormal mitosis to the acquisition of DNA damage. *J. Cell Biol.* **2012**, *199*, 871–881.
- (31) Vermes, I.; Haanen, C.; Steffens-Nakken, H.; Reutelingsperger, C. A novel assay for apoptosis. Flow cytometric detection of phosphatidylserine expression on early apoptotic cells using fluorescein labelled annexin V. *J. Immunol. Methods* **1995**, *184*, 39–51.
- (32) (a) Ly, J. D.; Grubb, D. R.; Lawen, A. The mitochondrial membrane potential ($\Delta\psi_m$) in apoptosis: an update. *Apoptosis* **2003**, *8*, 115–128. (b) Green, D. R.; Kroemer, G. The pathophysiology of mitochondrial cell death. *Science* **2004**, *305*, 626–629.
- (33) (a) Mollinedo, F.; Gajate, C. Microtubules, microtubule-interfering agents and apoptosis. *Apoptosis* **2003**, *8*, 413–450. (b) Chiang, N. J.; Lin, C. I.; Liou, J. P.; Kuo, C. C.; Chang, C. Y.; Chen, L. T.; Chang, J. Y. A novel synthetic microtubule inhibitor, MPT0B214, exhibits antitumor activity in human tumor cells through mitochondria-dependent intrinsic pathway. *Plos One* **2013**, *8*, 58953. (c) Romagnoli, R.; Baraldi, P. G.; Lopez-Cara, C.; Kimatrai Salvador, M.; Preti, D.; Aghazadeh Tabrizi, M.; Bassetto, M.; Brancale, A.; Hamel, E.; Castagliuolo, I.; Bortolozzi, R.; Basso, G.; Viola, G. Synthesis and biological evaluation of 2-alkoxycarbonyl-3-anilino benzo[b]thiophenes and thieno[2,3-*b*]pyridines as new potent anticancer agents. *J. Med. Chem.* **2013**, *56*, 2606–2618.
- (34) (a) Cai, J.; Jones, D. P. Superoxide in apoptosis. Mitochondrial generation triggered by cytochrome *c* loss. *J. Biol. Chem.* **1998**, *273*, 11401–11404. (b) Nohl, H.; Gille, L.; Staniek, K. Intracellular generation of reactive oxygen species by mitochondria. *Biochem. Pharmacol.* **2005**, *69*, 719–723.
- (35) Rothe, G.; Valet, G. Flow cytometric analysis of respiratory burst activity in phagocytes with hydroethidine and 2',7'-dichlorofluorescein. *J. Leukocyte Biol.* **1990**, *47*, 440–448.
- (36) Denault, J.-B.; Salvesen, G. S. Caspases: keys in the ignition of cell death. *Chem. Rev.* **2002**, *102*, 4489–4499.
- (37) Porter, A. G.; Janicke, R. U. Emerging role of caspase-3 in apoptosis. *Cell Death Differ.* **1999**, *6*, 99–104.
- (38) García-Sáez, A. J. The secrets of the Bcl-2 family. *Cell Death Differ.* **2012**, *19*, 1733–1740.
- (39) (a) Haldar, S.; Basu, A.; Croce, C. M. Bcl2 is the guardian of microtubule integrity. *Cancer Res.* **1997**, *57*, 229–233. (b) Poruchynsky, M. S.; Wang, E. E.; Rudin, C. M.; Blagosklonny, M. V.; Fojo, T. Bcl-xL is phosphorylated in malignant cells following microtubule disruption. *Cancer Res.* **1998**, *58*, 3331–3338.
- (40) Dubrez-Daloz, L.; Dupoux, A.; Cartier, J. IAPs: more than just inhibitors of apoptosis proteins. *Cell Cycle* **2008**, *7*, 1036–1046.
- (41) Romagnoli, R.; Baraldi, P. G.; Lopez Cara, C.; Kimatrai Salvador, M.; Bortolozzi, R.; Basso, G.; Viola, G.; Balzarini, J.; Brancale, A.; Fu, X.-H.; Li, J.; Zhang, S.-Z.; Hamel, E. One-pot synthesis and biological evaluation of 2-pyrrolidinyl-4-amino-5-(3',4',5'-

trimethoxybenzoyl)thiazole: an unique highly active antimicrotubule agent. *Eur. J. Med. Chem.* **2011**, *46*, 6015–6024.

(42) Viola, G.; Vedaldi, D.; Dall'Acqua, F.; Fortunato, E.; Basso, G.; Bianchi, N.; Zuccato, C.; Borgatti, M.; Lampronti, I.; Gambari, R. Induction of γ -globin mRNA, erythroid differentiation and apoptosis in UVA-irradiated human erythroid cells in the presence of furocoumarin derivatives. *Biochem. Pharmacol.* **2008**, *75*, 810–825.

(43) Porcù, E.; Viola, G.; Bortolozzi, R.; Mitola, S.; Ronca, R.; Presta, M.; Persano, L.; Romagnoli, R.; Baraldi, P. G.; Basso, G. TR-644 a novel potent tubulin binding agent induces impairment of endothelial cells function and inhibits angiogenesis. *Angiogenesis* **2013**, *16*, 647–662.

(44) Dorleans, A.; Gigant, B.; Ravelli, R. B.; Mailliet, P.; Mikol, V.; Knossow, M. Variations in the colchicine-binding domain provide insight into the structural switch of tubulin. *Proc. Natl. Acad. Sci. U. S. A.* **2009**, *106*, 13775–13779.

(45) *Molecular Operating Environment (MOE 2010)*; Chemical Computing Group, Inc: Montreal, Quebec, Canada, 2010; <http://www.chemcomp.com>.

(46) Korb, O.; Stützle, T.; Exner, T. E. PLANTS: Application of ant colony optimization to structure-based drug design. In *Ant Colony Optimization and Swarm Intelligence, 5th International Workshop, ANTS 2006, Brussels, Belgium, Sep 4–7, 2006*; Dorigo, M., Gambardella, L. M., Birattari, M., Martinoli, A., Poli, R., Stützle, T., Eds.; Springer: Berlin, 2006; LNCS 4150, pp 247–258.